

MONTANA RESEARCH AND ECONOMIC DEVELOPMENT INITIATIVE (MREDI)

Recovery of Metal Contaminants from Industrial Wastewaters with Magnetic Nanocomposites in a Novel Continuous Flow Process System

Final Report

Incorporating the Quarterly Progress Report for April 1 – June 30, 2017

Submitted to:

**Janelle Booth
Research Director
Montana University System
Office of the Commissioner of Higher Education**

Prepared by:

Jerome Downey, Professor, Montana Tech Department of Metallurgical and Materials Engineering (PI)

Edward Rosenberg, Professor, The University of Montana Department of Chemistry & Biochemistry (PI)

Hsin Huang, Professor, Montana Tech Department of Metallurgical and Materials Engineering (Co-PI)

Alysia Cox, Assistant Professor, Montana Tech Department of Chemistry and Geochemistry (Co-PI)

Katherine Zodrow, Assistant Professor, Montana Tech Department of Environmental Engineering

Submitted: July 14, 2017

RECOVERY OF METAL CONTAMINANTS FROM INDUSTRIAL WASTEWATERS WITH MAGNETIC NANOCOMPOSITES IN A NOVEL CONTINUOUS FLOW PROCESS SYSTEM

INTRODUCTION AND PROJECT SUMMARY

This final report covers the 21-month project performance period that extended from October 2015 to June 30, 2017. The project was completed within the allocated budget and each outcome and deliverable identified under the five major project objectives have been accomplished. The study highlights are presented herein but more detailed data related to the results described in this report as well as in the previous quarterly reports are available and will be provided on request.

In Fall 2015, the research team proposed to investigate a novel approach to resource recovery from wastewaters produced at various industrial manufacturing sites throughout Montana. The proposal built on pairing an industrially proven parent ion exchange (IX) synthesis technology developed by Dr. Edward Rosenberg at the University of Montana (UM) with a mechanically simple and relatively inexpensive continuous flow or “pipeline” IX reactor concept under development by Dr. Jerome Downey at Montana Tech (MTech). The combination of these innovative ideas represents a powerful technology for rapid continuous extraction of valuable and/or toxic metals from a broad range of contaminated waters and has potential to provide a cost-effective alternative to less flexible and less efficient technologies currently in use.

A schematic process flow diagram of the pipeline reactor system in its current state of development is presented in Figure 1. In the process, a slurry of magnetic nanocomposite IX particles with magnetic cores are mixed with the wastewater stream and the mixture is pumped through the reactor. Functional groups on the IX particle surfaces bond with metal ions as the particle-laden stream flows through the reactor. An electromagnet situated near the discharge end of the pipeline reactor captures and retains the magnetic nanoparticles without impairing the liquid flow. Periodically, valve positions are changed to divert liquid flow through a parallel magnetic module and the first electromagnet is de-energized to release the IX particles, which advance to a separate processing circuit wherein the metals are subsequently stripped from the particle surfaces with acid. The particles are chemically reconditioned and return to service in the pipeline reactor. The metals are concentrated in the acidic strip solution, which is processed for metal recovery via electrowinning; the metal-depleted solution is re-acidified and returns to the next stripping stage.

Two major challenges in this project were to develop a method for producing magnetically susceptible nanocomposite IX media and to design a reactor that is capable of loading the nanocomposite particles with metal and then capturing them before the treated water is discharged. Please note that copper was selected as the target metal in the initial experiments and that surrogate solutions were used in much of the development work to reserve the actual mine-affected samples for confirmatory tests.

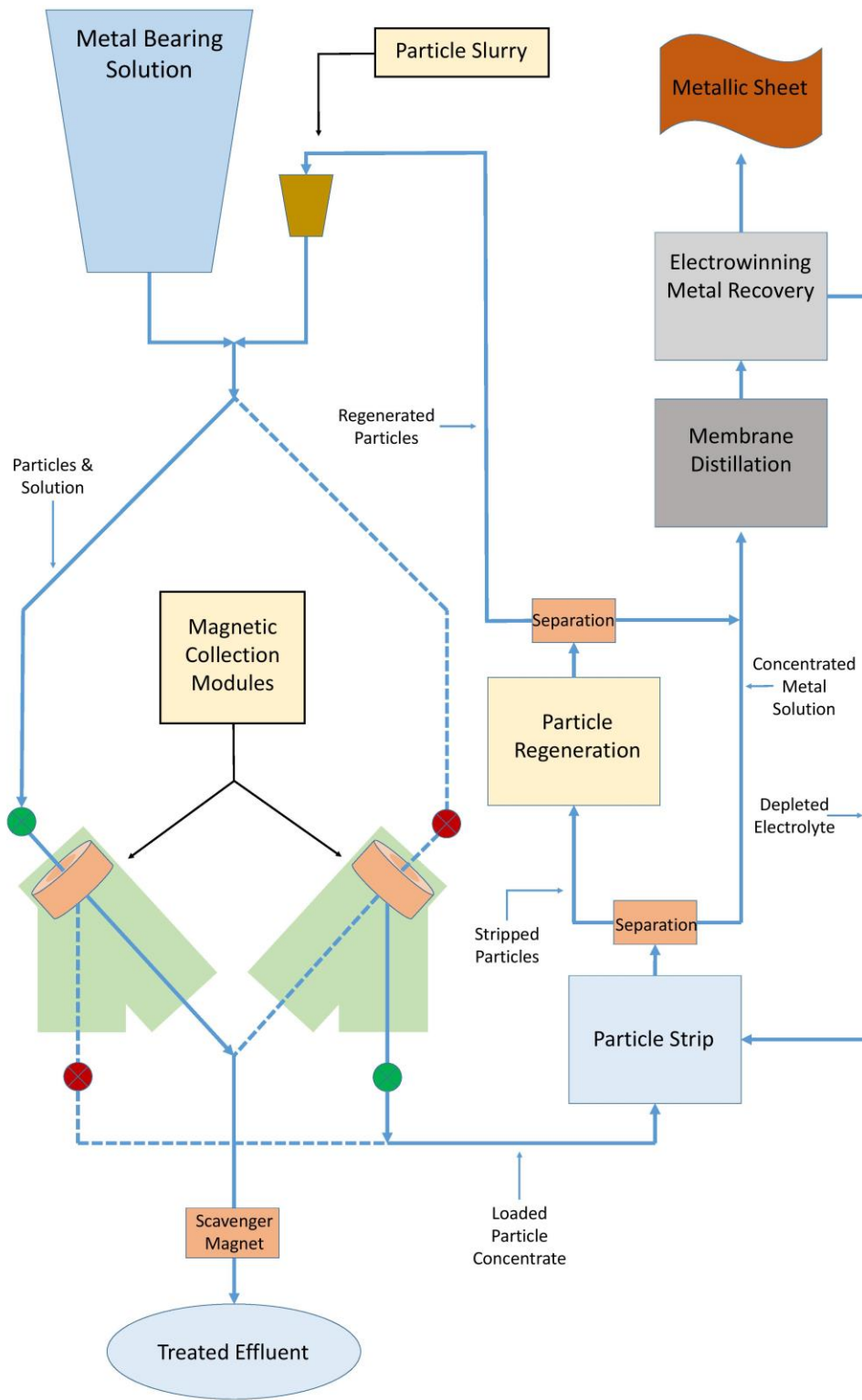


Figure 1 – Schematic process flow diagram for the continuous flow reactor system.

Dr. Rosenberg's research group at UM engaged in the synthesis of IX nanocomposite particles with magnetic cores. In general terms, the procedure involves a sequence of chemical processing steps. The first step involves the formation of relatively thin silica (SiO_2) shells around magnetite (Fe_3O_4) particles that have nominal diameters in the range of 20 to 30 nanometers (nm); the magnetite provides the necessary degree of magnetic susceptibility and the silica serves as a platform for organic molecules that will attract and bind with metal ions in the pipeline reactor. Next the silica coatings react with a mixture of organic chemicals (two silanes in a specific ratio). One of the silanes (TMCPS) acts as an anchor point for subsequent reaction with poly(allylamine) (PAA). In the final step, the PAA derivative is modified with sodium chloroacetate to give the desired amine acetate chelate ligand, which exhibits good copper capture at low pH.

The nanocomposite particles produced in Dr. Rosenberg's laboratory have a competitive copper loading capacity of approximately 0.5 millimoles per gram (mmole/g), a high surface area to volume ratio, and a loading rate that is ten times faster than that of comparable micro-scale ion exchange media. Metal recovery via stripping and particle regeneration have also been demonstrated to be highly effective and the IX particle life appears to be indefinite (similar micro-scale particles produced by Dr. Rosenberg's method last for thousands of cycles in industrial applications!). These characteristics translate to significant advantages and are considered to be critical to the successful operation of the pipeline reactor.

Reactor design, construction, and experimentation at MTech was conducted concurrently and in close collaboration with the nanocomposite development work at UM. Over the 7-quarter performance period of this project, two continuous flow reactor systems were designed, constructed, commissioned, and operated. The first of these systems features a much simpler design and substantially larger capacity (100-liter) and throughput (2 – 8 liters per minute) than previous laboratory-scale systems. The pipeline system now has no moving parts except for pumps and automatic valves; particles and fluids are well-mixed by creating turbulence via in-line static mixers. The design incorporates substantial technical advancements, most significantly the in-line water-cooled electromagnetic particle capture module. Under optimal operating conditions, a single module captures greater than 98% of the magnetite particles. The second system was designed and constructed after preliminary experiments with the nanocomposites revealed a persistent issue with particle agglomeration and settling in in the first reactor. While retaining the advantages of its predecessor, the newer 120-liter capacity reactor utilizes a vertical column and collection module to alleviate the particle agglomeration issue. More than 20 full-scale runs with a copper sulfate solution have been completed and the results are promising. Analysis of the depleted solution and strip solution suggest copper loading in excess of 0.5 mmole/gram, which is comparable to the loadings achieved in Dr. Rosenberg's laboratory. Research is shifting from surrogate solutions to real wastewater samples.

The culminating achievements of this research project include:

1. Successful development magnetic nanocomposite IX particles that have proved effective in both laboratory and pilot plant evaluations
2. The construction, commissioning, and operation of two pilot-scale continuous flow reactor systems, which will be used to further develop and demonstrate the process.
3. Identification and characterization of selected wastewater streams in Montana that are candidates for treatment via the magnetic nanocomposite/continuous flow reactor technology
4. Development and refinement of the process fundamentals, which will be incorporated in computational models and commercial scale-up efforts.

The technical advancements made during this project will enable project team members to confidently and aggressively pursue additional funding and industrial partnerships that are expected to lead to commercial implementation of the nanomaterials and reactor system.

ACCOMPLISHMENTS

This section of the report highlights specific accomplishments associated with each major project objective.

OBJECTIVE 1 – WASTEWATER CHARACTERIZATION

Dr. Alysia Cox (Co-PI), Assistant Professor
Montana Tech Department of Chemistry and Geochemistry

Ms. Renee Schmidt, Geochemistry M.S. Student (graduated May 2017)
Montana Tech Department of Chemistry and Geochemistry

Under the direction of Dr. Alysia Cox at MTech, the Laboratory Exploring Geobiochemical Engineering and Natural Dynamics (LEGEND) sampled several candidate wastewater streams at various Montana sites. In total, LEGEND secured 42 samples, which have been analytically characterized for metal content, pH, and other relevant parameters. Nine flooded underground mine complexes were sampled: Anselmo, Kelley, Steward, Ophir, Travona, Emma, Pilot Butte, Orphan Boy, and Orphan Girl. Additionally, the Horseshoe Bend water treatment plant and three wells, including wells tapping the high-copper Parrot tailings were sampled. A compendium of the sample characterization data is included in Appendix A (and previous quarterly reports).

The results of the wastewater sampling and analysis efforts validate the selection of copper, manganese, and zinc as principal target metals in laboratory and bench-scale evaluations as LEGEND detected significant concentrations of these metals in most of the samples; examples are provided in Figure 2. Large-volume samples for confirmatory testing in the pipeline reactor have been secured from the Berkeley Pit, Travona, Ophir, and Kelley mines, and the Parrot Tailings.

Inductively-coupled plasma optical emission spectroscopy (ICP-OES) has been the analytical method of choice for wastewater sample characterization. The method has proved to produce reliable data with acceptable accuracy and precision. This analytical method has been applied during portions of the study that relate to the other objectives.

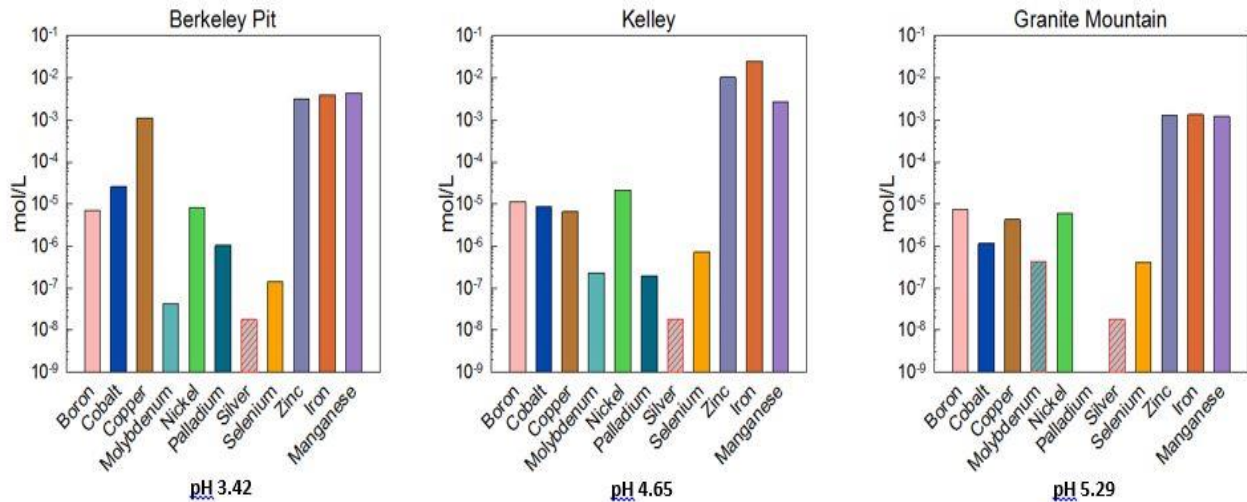


Figure 2 – Selected metal concentrations in three mine water samples.

OBJECTIVE 2 – MAGNETIC NANOPARTICLE SYNTHESIS

Dr. Edward Rosenberg (PI), Professor

The University of Montana Department of Chemistry & Biochemistry

Dr. Ryan Latterman, Post-doctoral Research Assistant

The University of Montana Department of Chemistry & Biochemistry

Mr. Emil DeLuca, Research Technician/Research Associate

The University of Montana Department of Chemistry & Biochemistry

Develop and optimize method(s) of producing magnetic nanoparticles to support ion exchange resin (Oct 2015 - Mar 2016)

Co-precipitation methods were explored using a range of ferrous and ferric salts. Well-formed magnetite crystals were obtained and they worked well with the subsequent chemistries. However, the particles were 5-15 nm in diameter and were not magnetic enough to be efficiently captured by the electromagnet in the pipeline reactor. The UM team then turned to a commercially available 20-30 nm magnetite particles made by SkySpring. These particles were also compatible with the subsequent chemistries and were 98% captured by the electromagnet. The particles did aggregate either before or after modification giving a nanomaterial that worked very well for the targeted applications. Dynamic light scattering experiments gave estimates of the hydrodynamic radius of 1-3 microns. Although this is much larger than we originally targeted they worked quite well.

Modify magnetic nanoparticles with polyamine and metal-selective ligands (Apr-Sep 2016)

The magnetite particles made in house by co-precipitation or using the SkySpring particles responded well to the proposed modification chemistries. The silica shell was applied using either silicic acid or tetraethylorthosilicate (TEOS). Both methods worked well but the TEOS method proved less complex and easier to modify. The second step involved reacting the silica shell with a mixture of trimethoxy(3-chloropropyl)silane (TMCPS) and trimethoxymethyl-silane (TMMS). Use of the mixture was based on prior results from modification of silica micro particles and the ratio was optimized for the magnetic nanoparticles (7 TMMS:1TMCPS). The TMCPS acts as an anchor point for the subsequent reaction with the polyamines, poly(allylamine) (PAA) and poly(ethyleneimine) (PEI). Both polymers gave acceptable metal ion capacities. PAA gave better capacities (0.5 mmol Cu/g) than PEI (0.2 mmol Cu/g) but PAA is more expensive. Final modification with sodium chloroacetate was achieved with the PAA derivative to give the amine acetate chelate ligand which showed the expected property of better copper capture at low pH.

Transmission electron microscope (TEM) and scanning electron microscope (SEM) images of the particles produced via this method appear in Figure 3. The individual particles tend to form larger agglomerates, as shown in the SEM image.

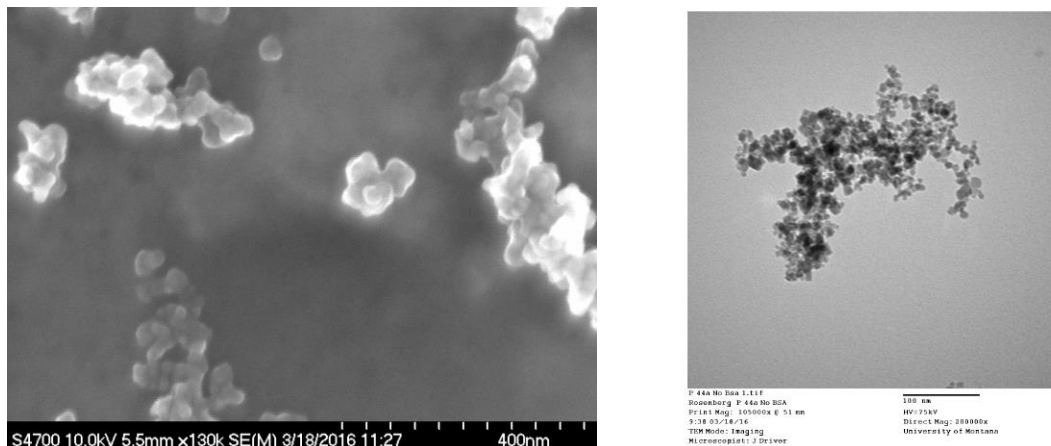


Figure 3 – At left, a TEM image of a Fe-Si-PAA core-shell nanoparticle and, at right a SEM image of a nanoparticle agglomeration.

Evaluate performance of the magnetic nanoparticles during bench-scale evaluation of the third-generation continuous flow reactor; modify nanoparticle configuration to achieve optimal reactor performance (Oct 2016 - Mar 2017).

The particles synthesized by the above-described methods were extensively evaluated at UM before passing them on to the MTech team. Kinetic analysis showed that these particles capture metal ion at rates ten times faster than related amorphous silica micro-particles; Figure 4 shows a loading curve generated with a 150 ppm Cu^{2+} starting solution.

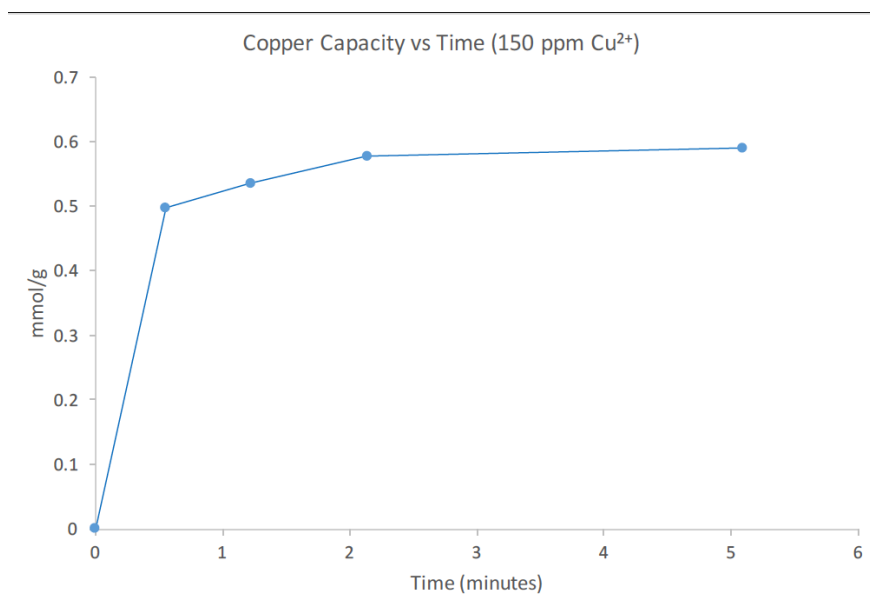


Figure 4 – copper ion capture rate from a 150 ppm Cu^{2+} solution. This loading rate is 10 times faster than that of micro-scale silica polyamine composite particles, which provides a definite process advantage.

Batches of particles were prepared from PAA at two molecular weights (3,000 and 60,000) and then loaded with copper, stripped and regenerated four times without loss of capacity. The corresponding copper capacities are plotted as a function of cycle number in the histogram in Figure 5. This finding illustrates the capability to repeatedly strip the metal ions and then regenerate the nanocomposite IX materials for reuse in the wastewater treatment process.

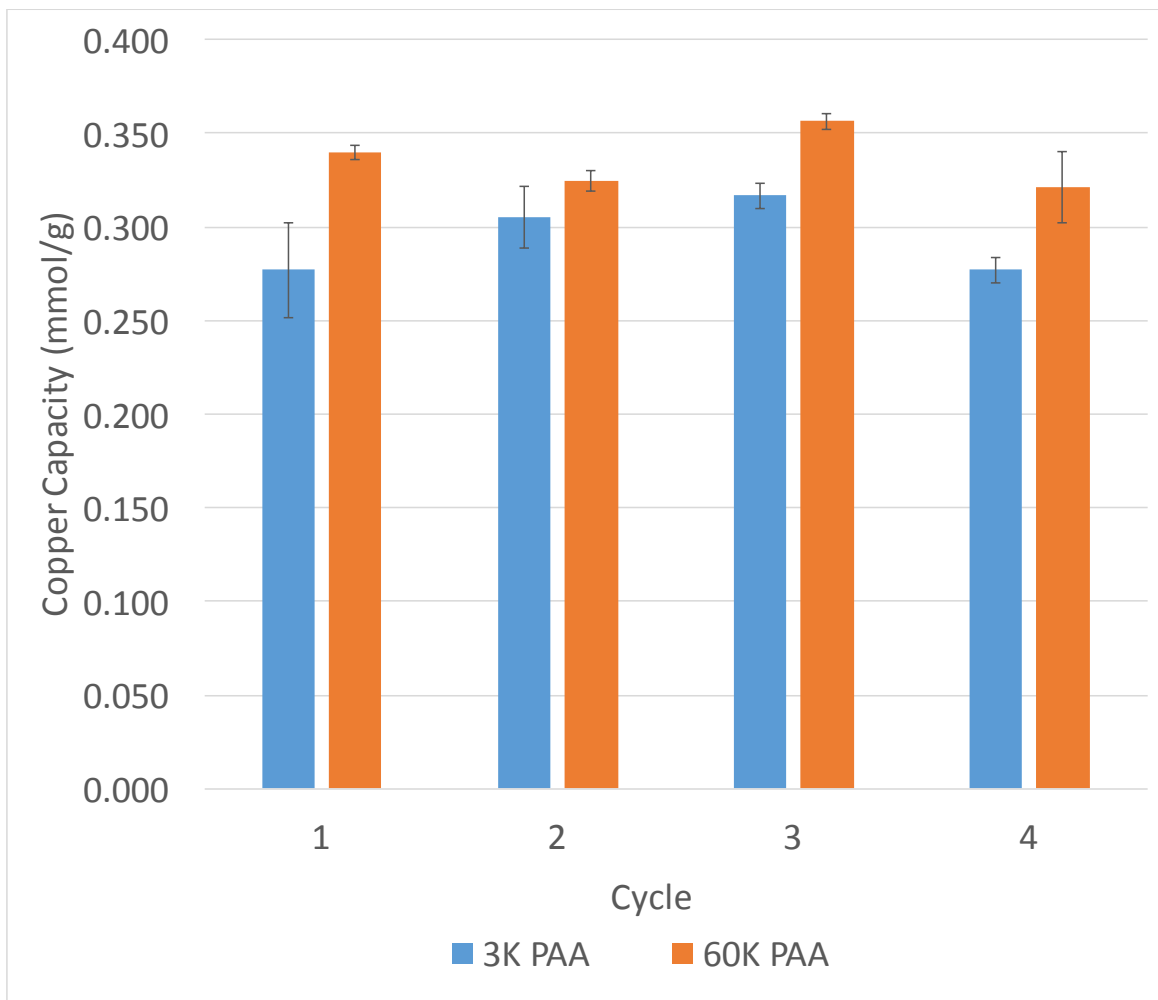


Figure 5 – copper capacities of CSMNs functionalized with 3,000 and 60,000 molecular weight PAA. The fact that the capacities did not diminish in successive cycles is an important and very favorable finding. Similarly prepared particles were reused ten times in the pipeline reactor without evidence of diminished loading capacity.

Scale-up of procedures to make 100 g batches of the materials (April 1, 2017-June 30, 2017)

Concentration isotherms were performed on the PAA derivate and tested against the Langmuir model. Excellent correlation coefficients (0.98) were obtained demonstrating that the particles are functioning as true ion exchange materials. During the final quarter of the grant period, a full time effort was put into optimizing the conditions for producing quantities of materials useful for the fourth generation pipeline reactor (100g). This effort entailed a redesign of the reaction equipment, reaction times and reagent quantities. In the end, the materials produced on this scale that had the same properties as the materials produced on the 5 g scale. These larger batches have been used extensively in the fourth generation reactor and it should now be possible to scale up even further.

Experimental determination of fundamental data related to performance of commercial ion exchange resins when applied to solutions bearing representative concentrations of the target metals (Oct 2015 - Mar 2016)

Experimental data on the performance of commercially available ion exchange materials was obtained by a thorough search of the literature. The more popular polystyrene materials had metal ion capacities in the range of 0.1 to 1 mmol of metal ion per gram of IX media, depending on use conditions, type of metal and functionality. The commercially available media have relatively slow capture kinetics relative to the nanoscale particles eventually produced in this project. The UM team has amassed a large amount of information on the pros and cons of the commercially available resins for comparison with the previously developed micro scale silica based materials. In general they have long usable lifetimes, but shrink and swell with swings in pH and are prone to fouling in organic containing waste streams and clogging when used in columns with feeds containing suspended solids. The target nanoparticles would circumvent most of these problems.

OBJECTIVE 3 – SECURE FUNDAMENTAL AQUEOUS PROCESSING DATA AND GENERATE PROCESS MODELS

Dr. H.H. Huang (Co-PI), Professor
Montana Tech Metallurgical and Materials Engineering Department

Ms. Maureen Chorney, M.S. Student
Montana Tech Metallurgical and Materials Engineering Department

The Objective 3 activities were mainly conducted to establish the theoretical bridge between Objective 2 (magnetic nanomaterial synthesis and development) and Objective 4 (pipeline reactor). The availability of reliable computational process models is invaluable to commercial process design and scale-up efforts. In addition to the obvious design considerations, models that are able to accurately predict system performance based on the selection of input parameters or “process conditions” can be used to guide operating decisions. If the models are proven to be extremely accurate, they are sometimes used in as feedforward algorithms in advanced process instrumentation and control systems.

To provide the theoretical framework for a detailed process model, Dr. H.H. Huang completed a fundamental study on the adsorption reaction for ion exchange media made from fine silica gel particles. Operating data generated during Objective 4 of this study are used to refine computational models that simulate the behavior of the magnetically susceptible nanocomposite materials within the continuous flow reactor system. The development of Dr. Huang’s theoretical framework can be traced through the succession of quarterly reports; his final report, “Fundamental Study: Adsorption Reaction for Ion Exchange Media made from Fine Silica Gel Particles,” is included in its entirety as Appendix B.

Limited equilibrium and kinetics studies were undertaken to develop data on resin performance to be used in the fundamental models. Samples of the magnetic nanoparticle IX material developed at UM and four commercial resins were obtained for purpose of comparison. Batch tests were performed to evaluate equilibrium conditions, and kinetic studies were conducted using a typical column setup, as well as agitated beaker tests. Rate constants and resin capacities were determined based upon literature models. The results, presented in Appendix C, confirm that the magnetic nanoparticles very rapidly load with the copper in dilute (~100 parts per million Cu^{2+}) wastewater solutions, which is precisely what these particles are designed to do.

Model refinement is an ongoing procedure. Further refinements will be based on the analytical characterization of the wastewater samples, experimental determination of fundamental data related to performance of IX resins when applied to solutions bearing representative concentrations of the target metals; and actual system performance as measured when the pipeline reactor is processing surrogate solutions and actual wastewater samples.

OBJECTIVE 4 – CONTINUOUS FLOW REACTOR DESIGN, CONSTRUCTION, COMMISSIONING, AND OPERATION

Dr. Jerome Downey (PI)

Professor of Extractive Metallurgy, Montana Tech

Mr. David Hutchins

Materials Science Ph.D. Candidate, Montana Tech

Concurrent with the reactor design and construction over the 7-quarter performance period of this project, two continuous flow reactor systems were designed, constructed, commissioned, and operated at MTech. In November 2015, the team began to design the first of these systems, which vastly simplified the reactor design while incorporating some substantial technical advancements. The 2-inch-diameter pipeline reactor has a 100-liter capacity and its flowrate (2 to 8 liters per minute) is much greater than the 1-centimeter-diameter and 1-inch-diameter laboratory reactors used in previous studies. The in-line, water-cooled electromagnetic particle capture module shown in Figure 6 represents a substantial advancement in reactor design that resulted in a simpler and more robust system. Within the system, the 6-inch diameter module is situated near the fluid discharge end of a 2-inch-internal diameter continuous flow reactor, which was constructed in a helical configuration (Figure 7) that incorporates static mixing. Under optimal low-flowrate operating conditions, the module has been demonstrated to capture greater than 98% of 20-30 nm diameter magnetite particles. An automated process control system governs all aspects of the reactor operation in addition to recording data through a graphical user interface.

Early experimentation with the pilot-scale reactor revealed a tendency for the magnetic nanocomposite particles to agglomerate and settle in the pipeline tubing. This finding led to the design and construction of a second pilot-scale reactor. As seen in Figure 8, this reactor utilizes a vertical column and collection module that is capable of handling the agglomerates without problems due to settling. The reactor is fully functional and the advantages of the previous prototype have been retained without compromise. More than 20 full-scale trials have been completed using a copper sulfate surrogate solution as the feed. The results are promising; analysis of the depleted solution and strip solution suggest copper loading of over 0.5 mmole/gram, which is comparable to the loadings achieved in Dr. Rosenberg's laboratory. The reactor effectively captures the magnetic particles at water flow rates of up to 8 liters per minute, which means that it already operates at a scale suitable for some low-volume, low-flowrate industrial applications.

Experimentation with real mine affected waters has been initiated and is currently underway at MTech. The experiments are being performed on samples secured from local mines, wells, and the Berkeley Pit. A trial utilizing a sample of groundwater from the Parrot tailings has been performed, and analysis is forthcoming. A glass reactor has been designed and ordered that will be implemented in tandem with the existing reactor. This arrangement, which is illustrated in Figures 8 and 9, allows for continuous operation and allow for visual inspection of the collection process.

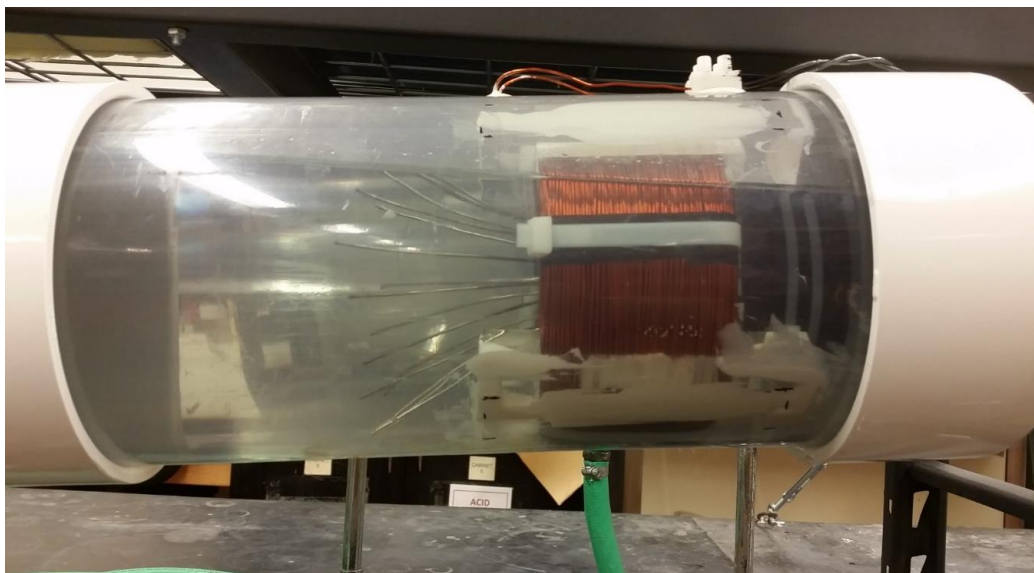


Figure 6 – a photograph of the first prototype in-line electromagnet module developed at Montana Tech during this project. When the reactor operates at optimal process conditions, this module consistently captures more than 98% of fine (20-30 nm diameter) magnetite particles as the water passes through.



Figure 7 – the 3rd generation continuous flow reactor. The white arrow in the photograph points to the in-line electromagnet module that captures and retains the magnetic nanoparticles without impeding the wastewater flow. This reactor has a 100 liter volume and solution flow rates range from 2 to 8 liters per minute.



HOW IT WORKS:

A slurry of magnetic nanocomposite ion exchange (IX) particles is introduced to the surrogate wastewater stream at the top of the platform.

Functional groups impregnated on the surfaces of the ion exchange particles bond with metal ions as the particle-laden stream flows downward through the reactor.

As the solution flows through the electromagnet module (the white wye in the photograph), the electromagnet retains the magnetic nanoparticles without impeding the wastewater flow. Treated water flows out of the angle leg of the wye

The valve positions are periodically changed to divert flow down through the vertical leg of the wye and into a collection receptacle (not shown).

The electromagnet is de-energized to release the particles, which are subsequently stripped, reconditioned, and returned to service. The strip solution is processed for metal recovery by electrowinning.

Figure 8 – Photograph of the pipeline reactor in the vertical configuration.

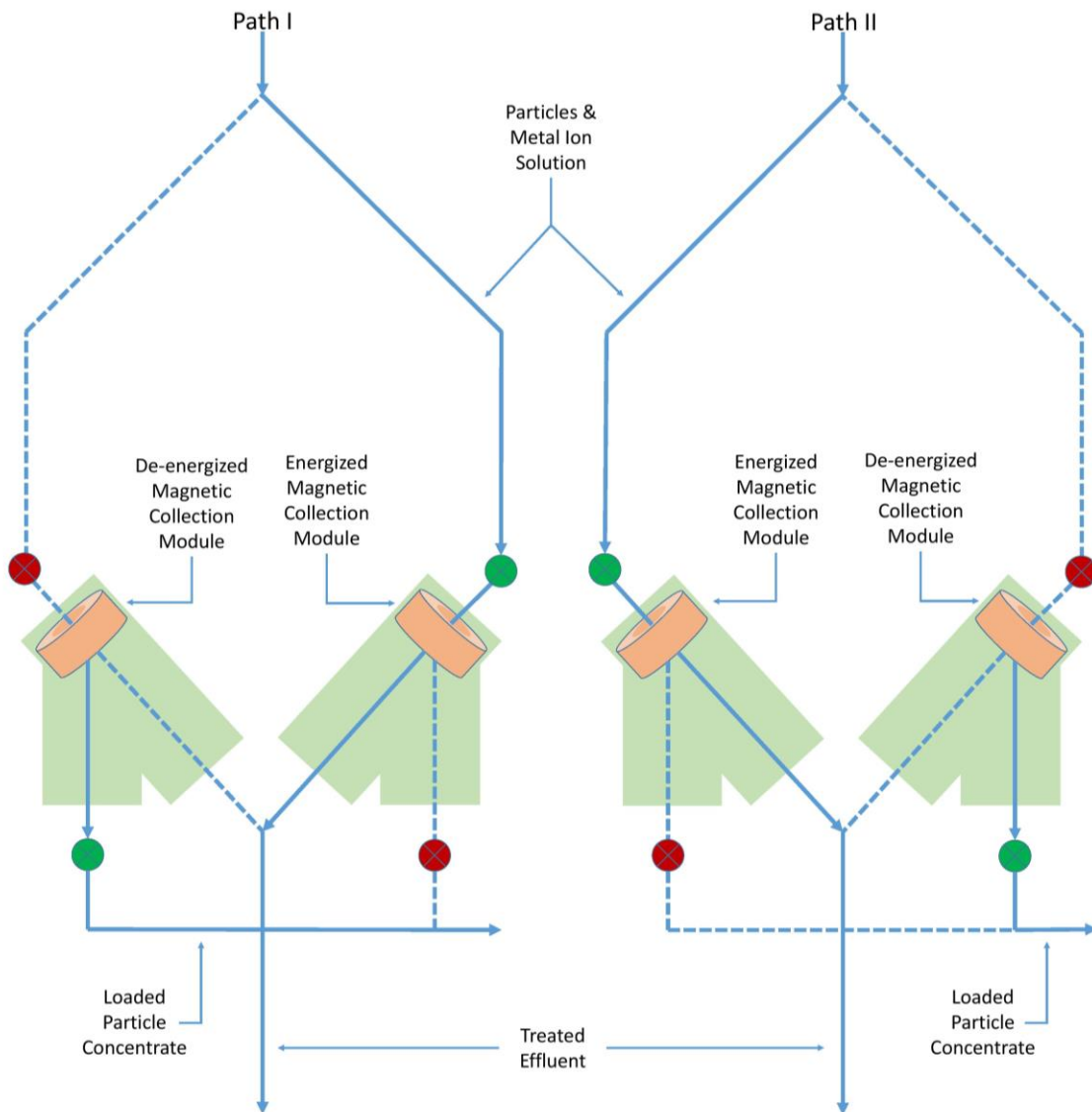


Figure 9 – Schematic of continuous flow arrangement. The valve arrangement alternates the flow through one module, then the other. In path I, the flow is directed through the energized magnetic collection module on the right where loaded particles are retained and the treated solution exits the system. In the module on the left of path I, the magnet is de-energized and loaded particles are released and routed to the stripping process. Periodically, as the magnetic collection reaches full loading, the process is reversed as seen in path II.

The emew® electrowinning system (Figure 10) was procured and commissioned to demonstrate metal reduction from IX strip solutions with low dissolved metal tenors. The emew® design is well-suited for processing the low-metal tenor strip solutions produced in the pipeline reactor. Copper and zinc recovery from surrogate solutions have been demonstrated. Coherent copper cathodes have been produced from starting solutions that have been depleted to levels below 1 gram per liter of Cu^{2+} ions.

In light of the low metal concentrations of some industrial wastewater contaminants determined from the Objective 1 results, concerns developed about the ability to adequately concentrate metal in the pipeline reactor strip solutions in preparation for electrowinning or other metal recovery methods. Dr. Katherine Zodrow and post-bac research assistant Christina Eggenperger joined the MTech project team to investigate membrane distillation (MD) as a method of further concentrating the metal in the pipeline reactor strip solutions in preparation for metal recovery via electrowinning. The report on their investigation is presented in Appendix D.



Figure 10 – the laboratory electrowinning circuit. Electrowinning is a means of recovering metals from solution by reducing the ions and plating high-purity metal on a cathode. In this circuit, the actual electrowinning occurs in the cylindrical column at center. At right, copper and zinc sheets electroplated from surrogate sulfate solutions

Electrowinning system performance parameters:	
Copper	40-45 °C electrolyte
	2.5V 11A
	94% current efficiency
Zinc	30-50 °C electrolyte
	5V 20A
	95.5% current efficiency

OBJECTIVE 5 – DATA CONSOLIDATION AND REPORTING

Data generated through the fulfillment of Objectives, 1, 2, 3, and 4 have been analyzed for presentation in this final report. These data are deemed suitable to form the design basis that will ultimately be used to design and operate commercial scale facilities for magnetic nanomaterial synthesis, continuous flow reactor manufacturing. The information developed through this study will be leveraged to attract additional funding from Federal Agencies with programs in which the continuous flow reactor are of interest.

- Documentation protocols, including laboratory notebook, file naming and sharing procedures, have been established and are in effect.
- The established project metadata accumulation, consolidation, and security measures remain in effect.
- Data have been presented in quarterly project status reports and in this final report.

LONG-TERM IMPACTS

This project is expected to generate a series of positive long-term impacts and activities that will extend beyond the original MREDI grant. This technology represents a potentially significant impact to the fields of wastewater treatment and hydrometallurgy and research with the reactor will continue into the foreseeable future. Applications to specific industrial challenges are being explored. Alternative applications of the technology are being explored, including the treatment of wastewater for anions, nutrients, and petroleum contamination.

Pending project completion, researchers at UM and MTech plan to present their findings by publishing in high-impact peer-reviewed journals, delivering presentations at professional society symposia, workshops, and short courses.

ADDITIONAL GRANT ACTIVITIES

LEGEND metrics include one BNRC grants (\$50,306) to Dr. Alysia Cox; the research will commence in August 2017 and continue through August 2019. A new partnership formed between the Montana Bureau of Mines and Geology (MBMG) and LEGEND.

Dr. Downey is engaged in the current EPSCoR Track 1 Proposal Science Writing Team. If the National Science Foundation funds the proposed research, Dr. Downey will be a co-PI and Dr. Rosenberg will be a technical advisor for a project that relates to the application of the magnetic nanocomposite/continuous flow reactor. The \$20 million proposal will be submitted to the National Science Foundation before the August 21, 2017 deadline.

A proposal is in preparation for the NSF program Biological and Environmental Interactions of Nanoscale Materials. The proposed research will focus on the nanocomposite materials developed under the MREDI grant, and their potential interaction in the environment.

PARTNERSHIPS FORMED

A partnership with Montana engineering firm Water and Environmental Technologies (WET) has been established for the advancement of research and commercialization under the Small Business Technology Transfer (STTR) program. WET is a private sector environmental services firm that specialized in water treatment and water treatment technologies. The initial grant application (to the National Science Foundation, NSF) was denied.

Multiple SBIR (Small Business Innovative Research) and STTR grant applications to various agencies with interests in water quality and/or wastewater treatment are planned. Target agencies include the United States Department of Defense, the Department of Energy, the Environmental Protection Agency, and the National Science Foundation, among others. In each of these projects, the current project team members will collaborate with industrial partners. In addition to securing funding for continued process development, the projects are expected to identify new applications and ultimately lead to commercial implementation.

NEW BUSINESSES/COMMERCIAL PRODUCTS DEVELOPED

To this juncture, no new Montana businesses have been created nor have any patents been awarded. However, the research has led to the development of intellectual property (the in-line electromagnet module, for example) and patent applications will be filed.

Recent presentations by Dr. Rosenberg and Dr. Downey elicited extremely favorable audience responses. Dr. Rosenberg presented an invited lecture at the 2017 meeting of "Macromolecular Architectures and Materials" in Sochi Russia June 6-10, 2017. Dr. Downey presented an invited lecture at the "Recycling Metals from Industrial Waste" short course and workshop in Golden, Colorado, June 27-29, 2017. Both presentations were well-received because the audiences judged that the technology is much closer to actual implementation than most of the other lectures presented. There were several enquiries about when our process would come on-line and a number of industry representatives came forward to discuss specific applications for the technology.

JOBS CREATED

Each of the participating faculty members received summer compensation for their contributions to the project:

1. Hsin Huang, Co-PI, Professor, Metallurgical and Materials Engineering (M&ME)
2. Alysia Cox, Co-PI, Assistant Professor, Chemistry and Geochemistry
3. Jerome Downey, PI, Professor, Metallurgical & Materials Engineering
4. Edward Rosenberg, PI, Professor, Chemistry and Biochemistry, University of Montana
5. Katherine Zodrow, Assistant Professor, Environmental Engineering

The following students were employed full-time or part-time during the course of this research project:

1. Ryan Latterman, Post-Doctoral Research Associate at UM
2. David Hutchins, Materials Science Ph.D. candidate at MTech
3. Renee Schmidt, Geochemistry M.S. student at MTech
4. Maureen Chorney, Metallurgical Engineering M.S. student at MTech
5. Christina Eggensperger, Environmental Engineering post-bac student at MTech
6. Jared Geer, M&ME undergraduate student at MTech
7. Elizabeth Raiha, M&ME undergraduate student at MTech
8. Auva Speiser, M&ME undergraduate student at MTech

Dr. Ryan Latterman (post-doc) and Mr. Emil DeLuca (research technician/assistant) were hired to assist Dr. Rosenberg in the development of the magnetic nanocomposite IX particles. Dr. Latterman has accepted a faculty position at an out-of-state college. Mr. DeLuca is attending graduate school out of state.

On May 22nd, Renee Schmidt successfully defended her MS in Geochemistry thesis entitled “Biogeochemical Interactions in Flooded Underground Mines.” The final version will be published on ProQuest in the middle of August. A manuscript based on Schmidt’s research will be submitted for publication in September 2017.

On June 22, David Hutchins successfully completed his doctoral candidacy examination. The work performed on the MREDI-funded project will be the subject of Mr. Hutchins’s dissertation, which is anticipated to be completed in Spring 2018.

The project has inspired students to participate in university-level research. A new Geochemistry MS student at Montana Tech has expressed interest in working on a similar topic after talking with David Hutchins. Christina Eggensperger, who entered the project as a post-bac student, is now enrolled as a M.S. student in Environmental Engineering.

The project funded undergraduate Senior Design teams from the Electrical Engineering Department and the Metallurgical and Materials Engineering Department at Montana Tech during AY2016-17.

APPENDIX A

WASTEWATER CHARACTERIZATION

Dr. Alysia Cox (Co-PI)

Assistant Professor, Montana Tech Department of Chemistry and Geochemistry

Ms. Renee Schmidt, M.S. Student (graduated May 2017)

Montana Tech Department of Chemistry and Geochemistry

The Laboratory Exploring Geobiochemical Engineering and Natural Dynamics (LEGEND) sampled local surface waters on seven different days (once every ~3 months, 6 sites per day) for a total of 42 samples since the beginning of the project. Nine flooded underground mine complexes have been sampled for water quality to date (Anselmo, Kelley, Steward, Ophir, Travona, Emma, Pilot Butte, Orphan Boy, and Orphan Girl). We have sampled the Kelley, Ophir, and Travona twice. In addition, we have also sampled the Horseshoe Bend water treatment plant and three wells, including wells tapping the high-copper Parrot tailings. The mines can be classified into three geochemical zones, ranging from low pH, high metals, low sulfide in the East Camp mines to high pH, lower metals, and high sulfide in the Outer Camp mines (Figures 1 and 2; Appendix A, Figures A-1 to A-3). Copper concentrations range from tens of nanomolal to micromolal (from less than 1 – 366000 ppb) in various Montana waters sampled (Figure 3).

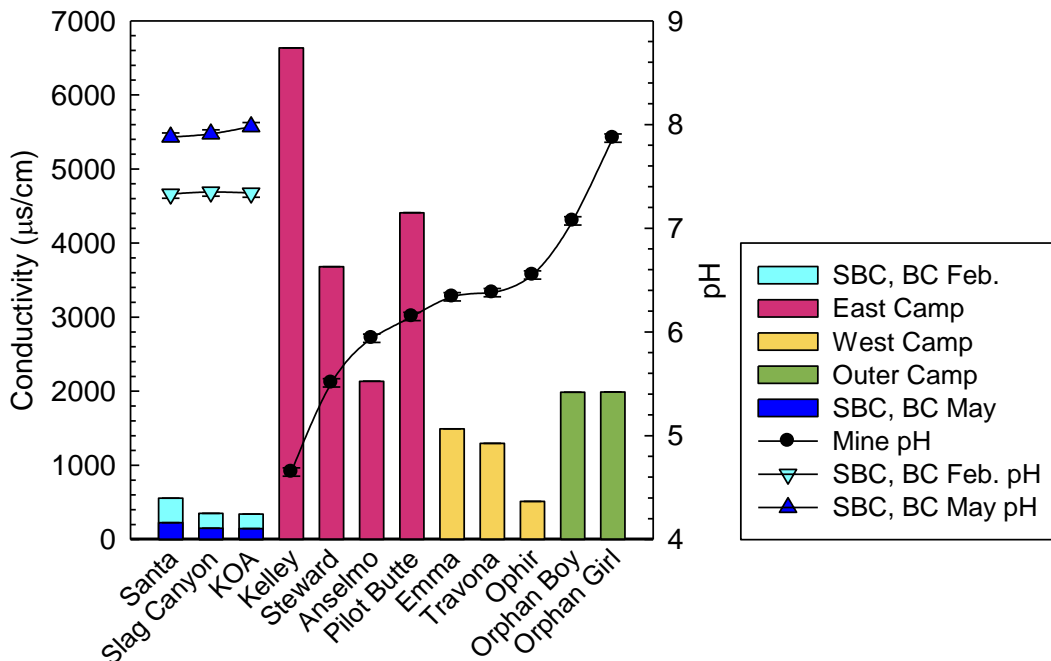


Figure A1: Conductivity and pH trends in Silver Bow and Blacktail Creeks and mines. Error bars on pH represents ± 0.05 from flux in meter readings. Conductivity error bars represent ± 1 $\mu\text{s}/\text{cm}$ from maximum flux in meter readings. Conductivity error bars are present but not visible due to scale (Schmidt and Cox, in prep).

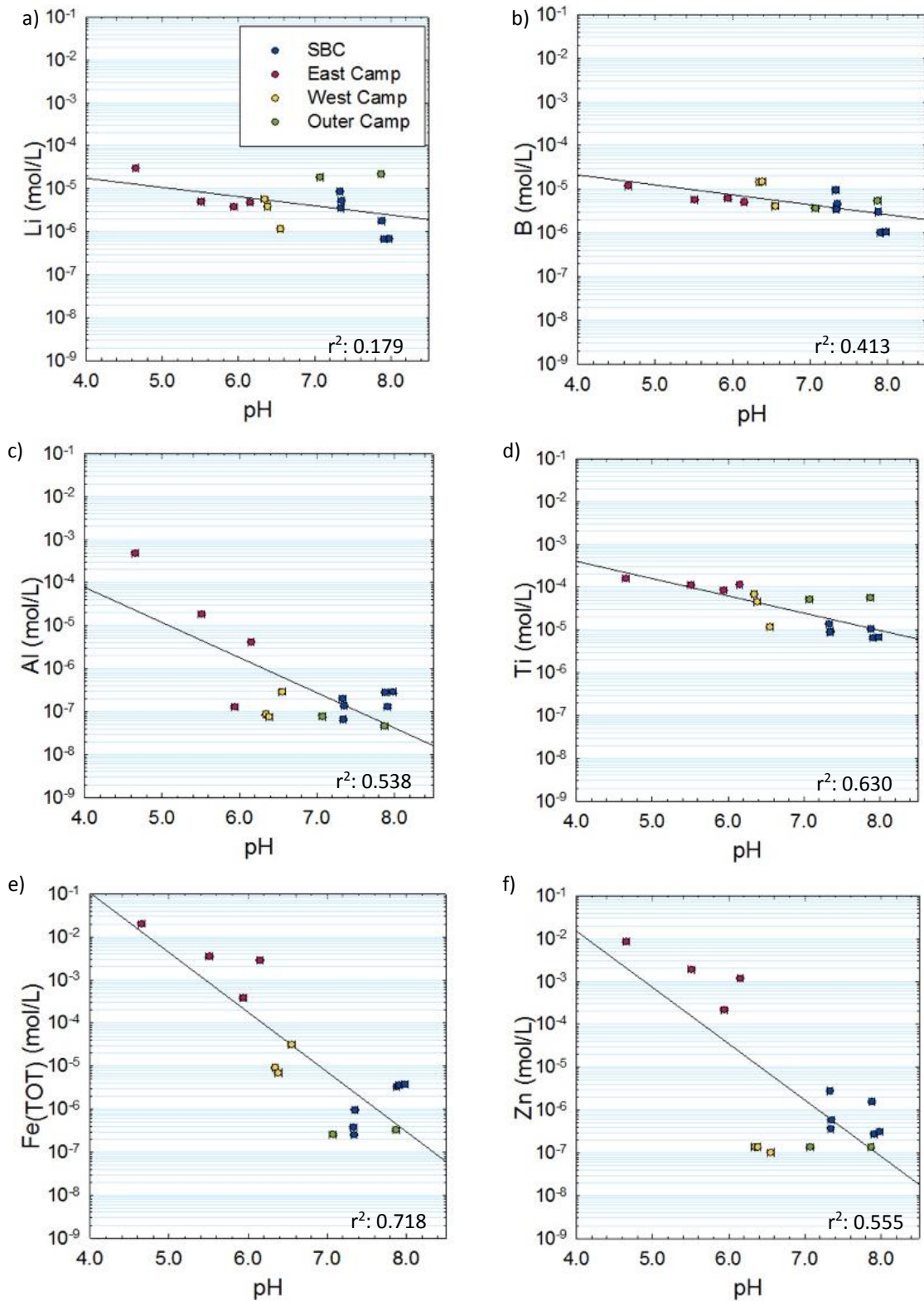


Figure A2.1: Total concentrations of elements vs. pH. Total concentrations of a) lithium, b) boron, c) aluminum, d) titanium, e) iron total, f) zinc, g) arsenic, h) strontium, and i) barium. Error bars represent All data obtained from ICP-MS. All concentrations on logarithmic scale (Schmidt and Cox, in prep).

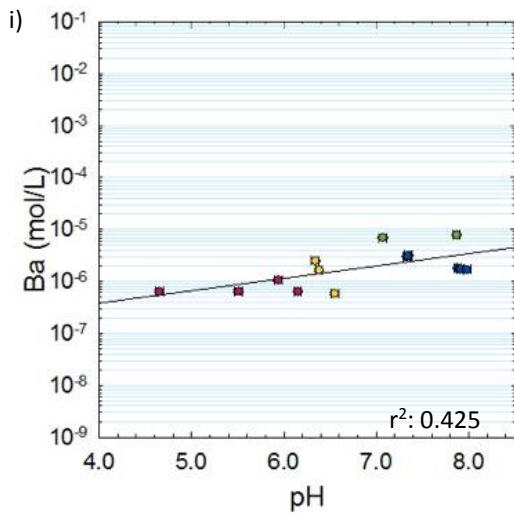
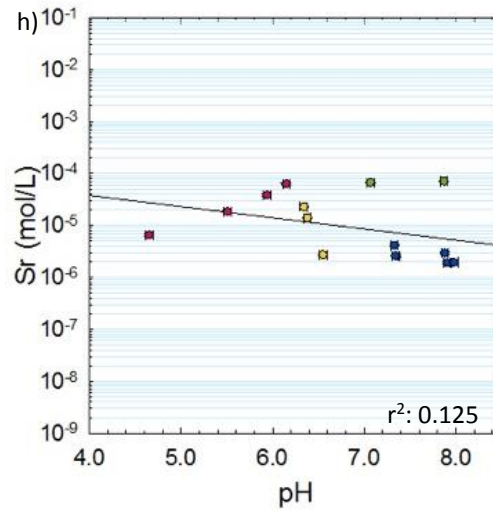
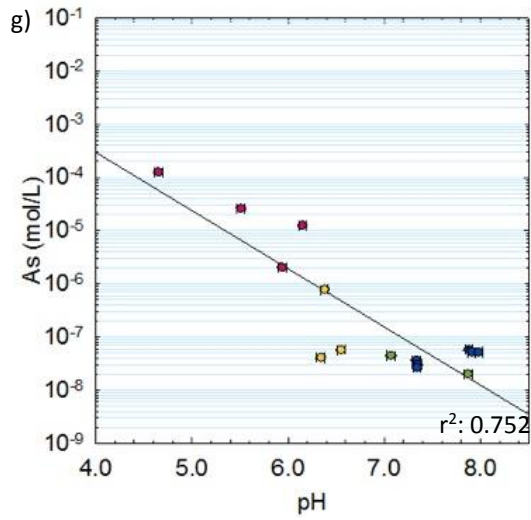


Figure A2.2: Total concentrations of elements vs. pH. Total concentrations of a) lithium, b) boron, c) aluminum, d) titanium, e) iron total, f) zinc, g) arsenic, h) strontium, and i) barium. Error bars represent All data obtained from ICP-MS. All concentrations on logarithmic scale (Schmidt and Cox, in prep).

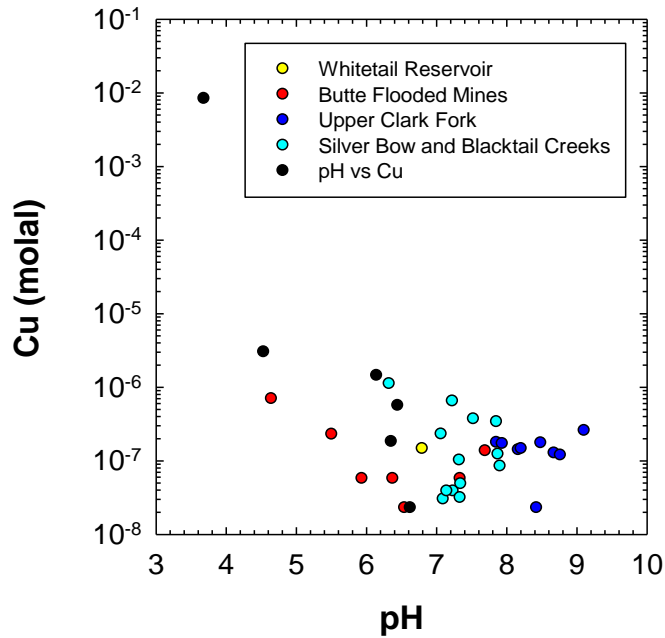


Figure A3: Total dissolved copper vs. pH for various Montana waters; the copper tenor ranges from less than 1 ppb to 366,000 ppb.

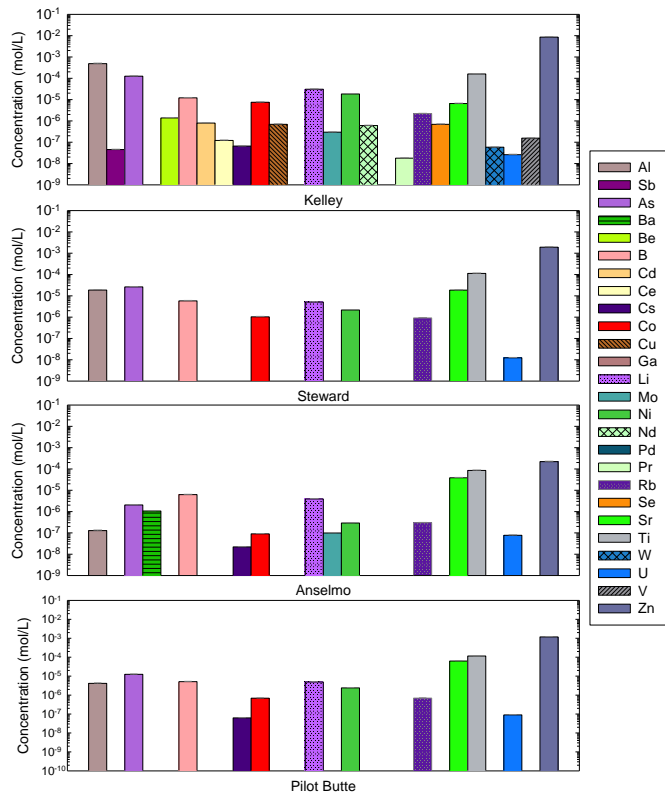


Figure A4.1 – Metal concentrations in Butte flooded mine shafts; East Camp trace element concentrations. The error bars represent instrumental error for each element. Detection limits vary by element. Concentrations reported in logarithmic values.

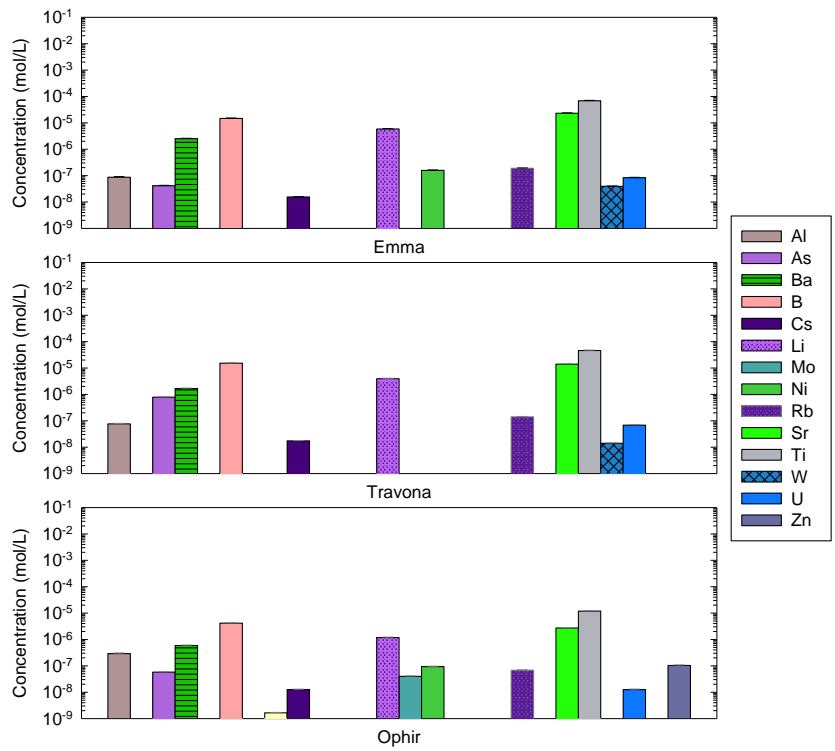


Figure A4.2 – Metal concentrations in Butte flooded mine shafts; West Camp trace element concentrations. The error bars represent instrumental error for each element. Detection limits vary by element. Concentrations reported in logarithmic values.

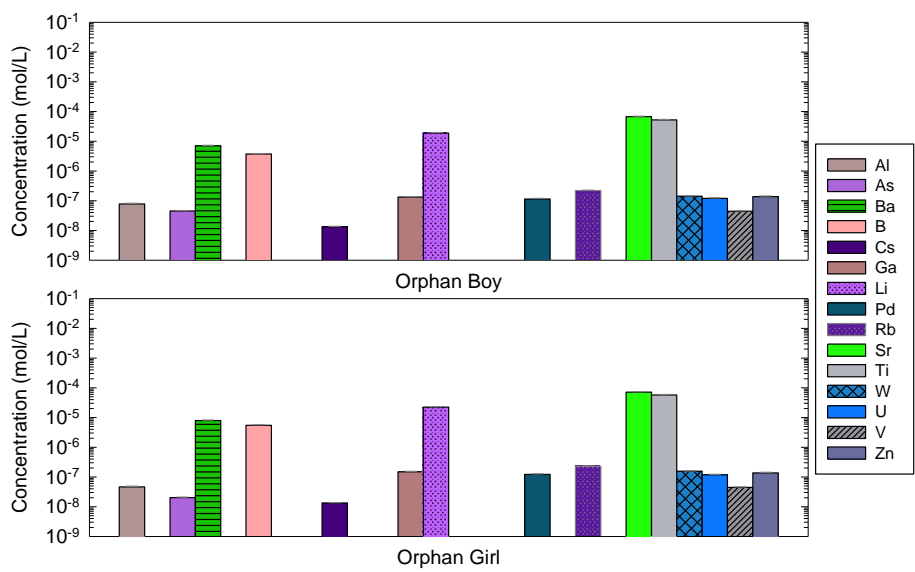


Figure A4.3 – Metal concentrations in Butte flooded mine shafts; Outer Camp trace element concentrations. The error bars represent instrumental error for each element. Detection limits vary by element. Concentrations reported in logarithmic values.

APPENDIX B

FUNDAMENTAL STUDY: ADSORPTION REACTION FOR ION EXCHANGER MADE FROM FINE SILICA GEL PARTICLES

Dr. H.H. Huang (Co-PI)

Professor, The University of Montana Department of Chemistry & Biochemistry

1. Introduction

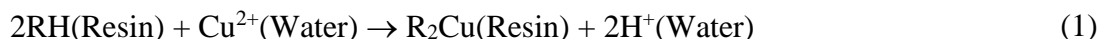
1.1 Basic concept

Ion exchange reactions involve the interchange of ions between an aqueous solution and insoluble solid resin. It is widely used to remove unwanted or toxic contaminants from water. It is also used in hydrometallurgical applications to concentrate and purify the metal values from leach solution. The exchange involves two parts:

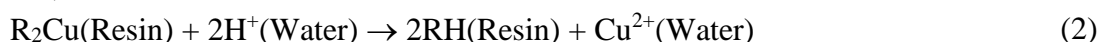
- The *resin base* can be a synthetic polymer, a silica polyamine composite (used in this research), or other stable and porous substances such as zeolite or clay.
- Functional molecules* are chemical permanently attached to the resin base. The functional molecules contain either cations or anions that are capable of exchanging similar type of ion from water.

The exchange operation involves two parts:

- Adsorption*: utilizes resin remove wanted (or unwanted) ions from the aqueous solution. Such as



- Elution*: recovers wanted ion to another water phase, and regenerate the resin to its original form. Such as,

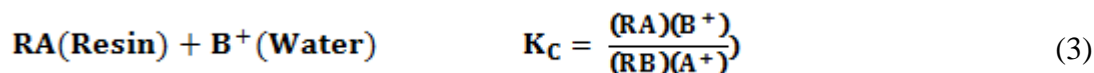


1.2 Silica Polyamine Composite

Professor Rosenberg's research group at the University of Montana has demonstrated the effective use of silica polyamine composite as an ion exchange resin. By employing different functional molecules, the resin can be used as a cation exchanger to remove heavy and precious metals [1] or as an anion exchanger for negatively charge ions such as As(III) and As(V) from water [2].

1.3 Basic reaction and equilibrium for adsorption reaction

The affinity of an ion exchanger for ions in the water differs. The affinity is usually represented by the equilibrium for a particular pH and temperature. As a generic example, the equilibrium constant (selectivity coefficient) between species A^+ and B^+ is:



For a non-specific exchanger, the order of cation affinities is normally (not a complete list) [3]: $\text{Ba}^{2+} > \text{Pb}^{2+} > \text{Cu}^{2+} > \text{Ca}^{2+} > \text{Zn}^{2+} > \text{Fe}^{2+} > \text{Mg}^{2+} > \text{K}^+ > \text{Na}^+ > \text{H}^+ > \text{Li}^+$.

The anion affinities are normally:
 $\text{UO}_2(\text{CO}_3)_3^{4-} > \text{ClO}_4^{4-} > \text{SO}_4^{2-} > \text{HAsO}_4^{2-} > \text{HSO}_4^- > \text{NO}_3^- > \text{Cl}^- > \text{HCO}_3^- > \text{CH}_3\text{COO}^- > \text{F}^-$.

In general, the ion exchanger tends to prefer counter ions of high valence (charge), and ions with the smaller hydrated diameter (volume).

1.4 Basic kinetics

As with any heterogeneous solid/liquid reaction, the kinetic of ion exchange reaction comprises many steps including the exchange reaction, diffusion into and out of the solid resin, and diffusion into and out of liquid film. Since each ion exchange system is different, researchers tend to describe the reaction mechanism, identify the rate controlling step, and finally formulate the rate equation.

1.5 Empirical equation for equilibrium and kinetics studies.

Due to complexity and challenges associated with applying parameters obtained from basic kinetic studies to the actual ion exchange operation, many researchers use empirical equations. For instance, the adsorption isotherm for equilibrium and breakthrough curves for column reaction presented by Professor Rosenberg [1, 2]. Experiment setup and formulation of those equation from results will be discussed in detail. All discussions assume that species A^+ is to be exchanged (adsorbed) onto the resin as shown by Equation 3.

2. Agitated Batch Study

2.1 Kinetics Study

This type of kinetic study is carried out in an agitated batch reactor. Depending on the reaction order, the rate equation is expressed by amount of A^+ removed per weight of exchanger at a given time, q_t , are:

1. Pseudo first order reaction where k_1 being the first order rate constant,

$$\ln(q_e - q_t) = \ln(q_e) - k_1 t \quad (4)$$

2. Pseudo second order reaction where k_2 being the second order rate constant,

$$\frac{1}{(q_e - q_t)} = \frac{1}{q_e} + k_2 t \quad (5)$$

3. Elovich model where a and b are constants,

$$q_t = \frac{1}{b} \ln(ab) + \frac{1}{b} \ln(t) \quad (6)$$

where q_e represents the amount of A^+ removed at equilibrium state.

Example system: Adsorption of Ni(II) and Pb(II) by Amberjet 1200 from Rohm&Hass [4].

From the linear plot of $\ln(q_e - q_t)$ versus t , based on Equation 4, the kinetics of Ni(II) and Pb(II) by Amberjet 1200 proved to follow the pseudo first order kinetic model, shown in Figures B1 and B2. Rate constant k_1 , will be negative slope from the plots.

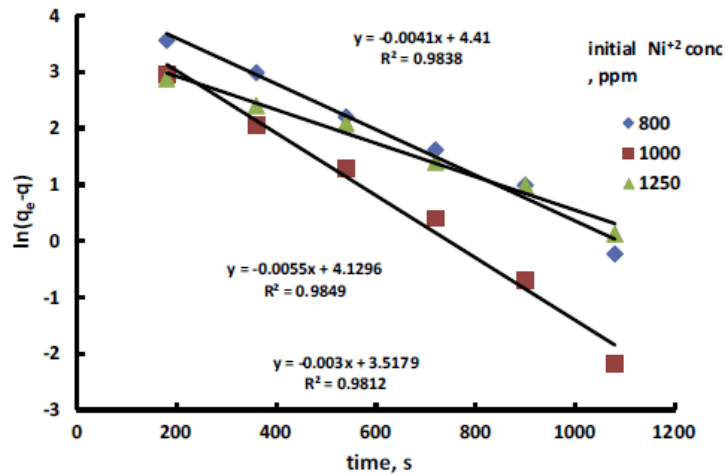


Figure B1: First order linear plot of Ni(II) adsorption by Amberject 120

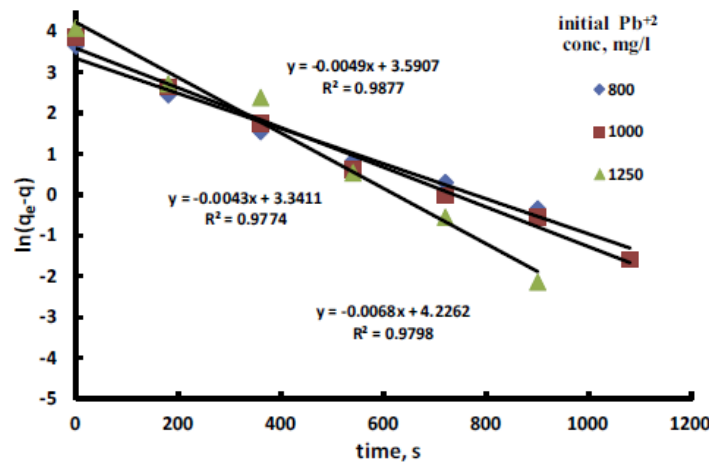


Figure B2: First order linear plot of Pbi(II) adsorption by Amberject 120

2.2 Equilibrium study – adsorption isotherm

The adsorption isotherm studies the partition of a species A between the solution and the exchanger under the equilibrium condition in Equation 3.

Example system: For numerical expressions of the isotherm, equilibrium study from Professor Rosenberg are used [2]. Briefly the study used the immobilized Zr(IV) on BPAP (phosphonic acid modified silica polyamine composite) resin to exchange As(V) and As(III) from the aqueous solution.

2.2.1 Adsorption reaction, Equilibrium Constant and adsorption isotherm

Symbol $S\equiv$ represents surface site that is capable of adsorbing species A from the solution to form $S\equiv A$ on the surface. The adsorption reaction is $A(aq) + S\equiv \leftrightarrow S\equiv A$ and equilibrium constant is

$$K(\text{ads}) = \frac{[S \equiv A]}{[S \equiv] \times [A]} \quad (7)$$

where the symbols $[S \equiv]$ and $[S \equiv A]$ denote the surface concentration of empty site and the site occupied by adsorbate A respectively; the symbol $[A]$ represents the concentration of adsorbate in the solution phase.

The adsorption isotherm is commonly practiced to investigate the equilibrium relationship between $[S \equiv A]$ and $[A]$. Take As(V) study for instance, the amount of As(V) adsorbed, $[S \equiv \text{As(V)}]$, was determined by measuring equilibrium concentration of $[\text{As(V)}]$ in the solution at pH 6, see Figure B3.

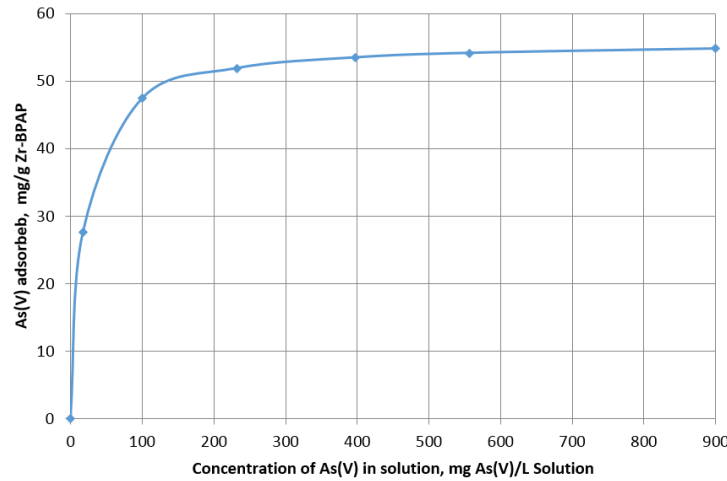


Figure B3. Adsorption isotherm of As(V) by Zr-BPAP at pH 6 replotted from data from Rosenberg [2].

2.2.2 Langmuir and Freundlich adsorption isotherms

Langmuir and Freundlich models are commonly used to formulate the experimental isotherm. The Langmuir hypothesis assumes the surface of adsorbent is homogenous and the maximum capacity can be expressed as the sum of empty and occupied sites as

$$[S \equiv T] = [S \equiv \text{max}] = [S \equiv] + [S \equiv A] \quad (8)$$

Where $[S \equiv \text{max}]$ can be evaluated from experimental data. The linear equation and derivation to estimate parameters for the model from laboratory tests is shown in detailed in section 2.2.3.

The Freundlich model applies to heterogeneous surface where maximum capacity cannot be achieved

$$[S \equiv A] = m [A(\text{solution})]^n \quad (9)$$

Where m and n parameters need to be evaluated from experiments. The linear equation to estimate the parameters for the model is

$$\ln[S \equiv A] = \ln(m) + n \ln([A(\text{solution})]), \quad (10)$$

Judging from adsorption isotherm of Figure 3, the Langmuir model seems to be a better model for As(V) adsorption by Zr-BPAP. The following uses Langmuir model for treating the example system.

2.2.3 Monolayer and Langmuir adsorption

As seen in Figure 3, the adsorption approaches a maximum at high equilibrium concentration of As(V). This is a typical indication of the monolayer adsorption, and is commonly explained by Langmuir adsorption model. From equilibrium constant, K (Equation 7) $[S \equiv]$ can be replaced by $[S \equiv T] - [S \equiv A]$, where the new symbol $[S \equiv T]$ represents the maximum coverage by the species A. Rearrangement of the equilibrium equation gives

$$s(T) + \frac{[A]}{[S(T)]} \quad (11)$$

Replacing $[A]$ with C_e , $[S \equiv A]$ with Q_c , $[S \equiv T]$ with Q_m , and K with K_{ads} , a straight line equation based on Langmuir model between C_e/Q_c and C_e can be obtained, presented by Professor Rosenberg,

$$\frac{C_e}{Q_c} = \frac{1}{K_{ads} Q_m} + \frac{1}{Q_m} C_e \quad (12)$$

Figure B4 is the Langmuir linear plot for As(V) adsorption by Zr-BPAP at pH6. The excellent fit of the model can be observed from experimental results. Constants Q_m and K_{ads} can be computed from the slope and intercept of the straight line equation.

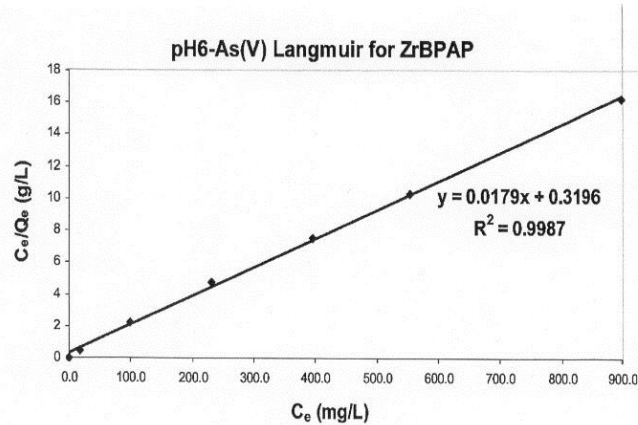


Figure B4. Linear plot based on Langmuir model for As(V) adsorption by Zr-BPAP from Rosenberg.

Using results from linear regression, $K_{ads} = 0.018$ L/g and $Q_m = 56$ mg/g for pH = 6.

2.2.4 Langmuir adsorption for competitive ions

As presented in the previous report, adsorption depends strongly with the equilibrium between the concentration of the ions in the aqueous phase and the amount adsorbed. The hypothesis of Langmuir adsorption model assumes the surface sites are limited only to a monolayer. The equilibrium equation is

$$\frac{K[A]}{1 + K[A]} \quad \text{or} \quad \Gamma_A = \frac{C_{\max} K[A]}{1 + K[A]} \quad (13)$$

Where K is the equilibrium constant, [A] is the concentration in the solution and [S≡A] is surface site occupied by species A having the unit such as moles adsorbed /m² of surface. It turns out that the new variable Γ_A (moles adsorbed / mass of adsorbent) would be easier to understand and determine.

When several different ions are present in the solution, the ions must compete to occupy the only available adsorbent surface sites. According to W. Stumm [5] and assume Species B is competing with Species A, the amount of A adsorbed will become

$$\Gamma_A = \Gamma_{\max} (K_A [A]) / (1 + K_A [A] + K_B [B]) \quad (14)$$

Where K_A and K_B are the equilibrium constants for species A and species B, respectively. The equilibrium constant values can be independently measured from the experiment. The formula can be expanded for more competitive ions.

3. Ion Exchange Column – study and design

3. 1 Introduction of Ion Exchange operation

Most ion exchange (IX) operations use packed bed columns. The mass (M) of the resin required depends not only on the solution flow rate (Q), and concentration (C₀) but also the resin's capacity to extract (q₀) and the kinetics constant of exchange reaction (k₁). The breakthrough curve is one of the key factors for the design of the column. It starts at the time (or volume of solution introduced) when metal (or pollutant) starts to leak out of the column until the exchanger in the column is totally exhausted. In Figure 5, MTZ stands for mass transfer zone where the active adsorption reaction is taking place.

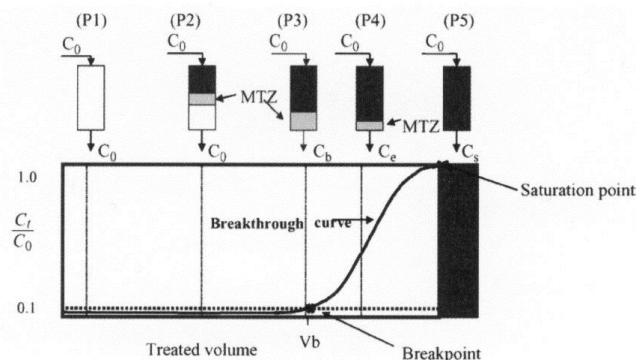


Figure B5. A typical breakthrough curve from an ion exchanger column operation [6]

3.2 Formulating the Breakthrough Curve – Thomas Model

The Thomas [7] model is one of the commonly cited mathematical equations used to formulate the breakthrough curve. The equation is simple and expressed for the concentration ratio between input (C₀) and output (C_t) as a function of time (t) or total volume introduced (V). Other parameters

include exchanger capacity (q_0) and kinetics constant (k_1), and operating conditions including the exchanger mass (M) and solution flow rate (Q).

$$\ln\left(\frac{C_0}{C_t} - 1\right) = \frac{k_1 q_0 M}{Q} - \frac{k_1 C_0 V}{Q} \quad \text{where } V = Q \times t \quad (15)$$

Example system: data from Ca^{2+} adsorption from a K_2CrO_4 aqueous solution by Amberlite IRC 748 are used for brief demonstration [8] in the following sections.

Unuabonah [9] summarized other ion exchange column operation models, including Adams-Bohart, Yoon-Nelson, and Clark.

3.2.1 Estimating exchange capacity q_0 and k_1 from experimental data

The capacity and the kinetics constant can be evaluated from the experimentally breakthrough curves obtained. According to Equation 15, a linear relationship between $\ln(C_0/C_t - 1)$ and V (or t) can be observed see Figure B6. Parameters, q_0 and k_1 , can be computed from the slope = $-k_1 C_0/Q$, and intercept = $k_1 q_0 M/Q$ of the straight lines.

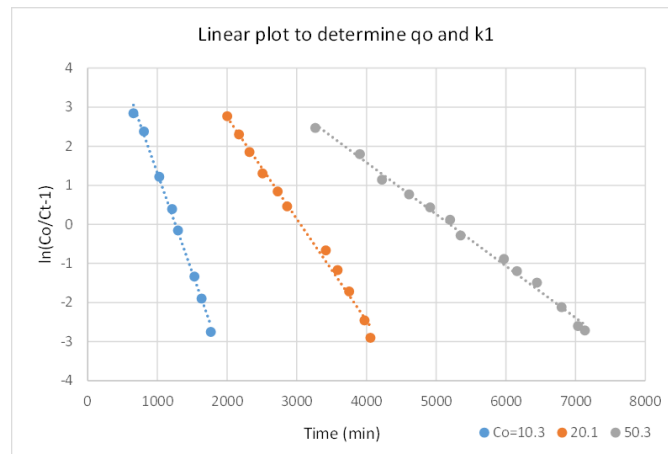


Figure B6: Linear plot to estimate exchange capacity, q_0 and kinetic constant, k_1 .

3.2.2 Predicting the Breakthrough Curve for giving Conditions

Once the exchange capacity and rate constant have been obtained, the breakthrough curves versus volume flow rate (or time) can be computed using Equation 16 (derived from Equation 15). The operation conditions such as the influent concentration, (C_0), mass of exchanger (M) and solution flow rate Q can be varied and implemented to the equation. Experimental data and model prediction under 3 different Ca^{2+} concentrations taken from Reference 8 are shown on Figure 7.

$$\frac{C_t}{C_o} = \frac{1}{\left(1 + \exp\left(\frac{k_1 q_o M}{Q} - \frac{k_1 C_o V}{Q}\right)\right)} \quad (16)$$

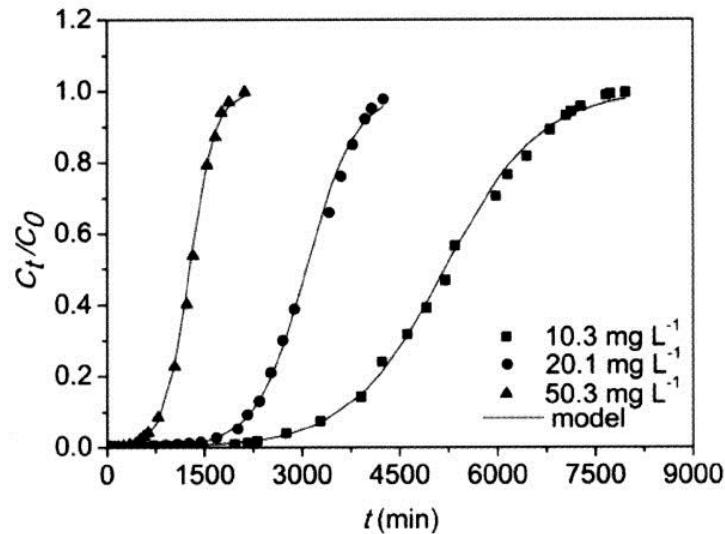


Figure B7: The model predicted the breakthrough curves versus points from 3 different experiments.

3.2.3 Design for the operation

The design of column is normally concentrated on total amount of resin needed for getting $C_t/C_o = 5\%$ (or 10%) from the breakthrough curve. The curve is constructed using Equation 16 by including all other required conditions and parameters estimated from performed experiments to the actual operation.

4. References

1. Rosenberg E.; et al., Metal Coordination and Selectivity with Oxine Ligands Bound to Silica Polyamine Composites,” Silica Polyamine Composites, *J. Appl. Polymer Sci.* 115, 2855-2864 (2010).
2. Rosenberg E.; et al., Characterization of Surface-Bond Zr(IV) and Its Application to Removal of As(V) and As(III) from Aqueous System Using Phosphonic Acid Modified Nanoporous Silica Polyamine Composites, *Ind. Eng. Chem. Res.*, 48(8), pp 3991-4001 (2009).
3. Clifford D., Chapter 9: Ion Exchange and inorganic Adsorption, Water Quality and Treatment A Handbook on Drinking Water Six edition, J.K. Edzwald editor by American Water Works Association (2010).
4. Zewail T.M.; Yousef N.S. Kinetics study of heavy metal ions removal by ion exchange in batch conical air spouted bed, *Alexandria Engin. J.*, 54, 83-90 (2015).
5. Stumm W., Chemistry of the Solid-Water Interface, Processes at the Mineral-water and Particle-Water Interface in Natural System, A Wiley-Interscience Publication (1992).

6. Tochohanoglous G.; et al., *Wastewater Engineering, Treatment, Disposal and Reuse*, McGraw-Hill, New York, (1991).
7. Thomas H.C., Heterogeneous ion exchange in a flowing system, *J. Am. Chem. Soc.* 66, 1664-1666 (1944).
8. Yu Z.; et al., Application of mathematical models for ion-exchange removal of calcium ions from potassium chromate solutions by Amberlite IRC 748 resin in a continuous fixed bed column, *Hydrometallurgy*, 158 165-171 (2015).
9. Unuabonah E.I.; et al., Predicting the dynamics and performance of a polymer-clay based composite in a fixed bed system for the removal of lead(II) ion, *Chemical Engineering Research and Design*. 90, 1105-1115 (2012).

APPENDIX C

DEVELOPMENT OF BASELINE ION EXCHANGE PARAMETERS

Dr. H.H. Huang (Co-PI)

Professor, The University of Montana Department of Chemistry & Biochemistry

Ms. Maureen Chorney

M.S. Student, Montana Tech Metallurgical and Materials Engineering Department

Equilibrium and kinetics studies were undertaken to provide supplement data on resin performance to be used in the fundamental models. Samples of the magnetic nanoparticle IX material developed at the University of Montana and four commercial resins were obtained for purpose of comparison. Batch tests were selected to evaluate equilibrium conditions, where sufficient time was allowed for resin to contact solution. Kinetic studies were conducted using a typical column setup, as well as agitated beaker tests. Rate constants and resin capacities were determined based upon literature models.

Experimental Methods

Batch testing was conducted utilizing five resins: Purolite® S930PLUS, Purolite® S940, Purolite® PFC100, Purolite® Purofine® PFC104Plus, and the University of Montana (UM) magnetic nanoparticles (MNP). The batch tests were performed in 20 mL glass scintillation vials. Varying amounts of each resin (100mg, 200 mg, or 400 mg) were weighed into each vial. Three copper solutions were prepared at a concentration of 60 mg/L of copper, using copper sulfate; each scintillation vial was filled with 20 mL of solution. Two solutions were buffered with a 0.1 M citrate buffer to create solutions of pH 5.4 and 6.2; the third solution was not buffered. A total of 45 sample vials were placed on an oscillating shaker table (480 rpm) for 20 hours.

The kinetics of resin loading was experimentally investigated using an up-flow column method for S930, S940, and PFC100. A bed volume of 4 mL was utilized for each of the three resins. The resin was contained between two polyethylene frits (MDPE, 0.059” – 0.079”) to ensure that undesired bed movement did not occur; small glass beads were used to fill the remaining space of the column. The packed column was rinsed with 18 M Ω de-ionized water before and after running 50 mL of 1000 mg/L copper solution through the column. Approximately 2.0 mL aliquots were collected, resulting in a total of 25 samples per resin.

The kinetics of the magnetic nanoparticle resin were analyzed using beaker tests. Approximately 3.0 grams of resin was used for each test. An oscillating shaker table (160 rpm) was employed to agitate the resin once the solution was added to the beaker. Three batch tests were conducted, varying only solution concentration (500, 1000, and 1500 mg/L Cu). Samples of approximately 4.0 – 5.0 mL were taken via syringe every 60 seconds once 200 mL of copper solution was added to the beaker. Samples were taken every 30 seconds for the first two minutes for the 1000 and 1500 mg/L beaker tests, with normal sample collection resuming after the two minute mark.

Experimental Results

The results of the batch tests are shown in Table 1. The solutions from each vial were analyzed by ICP to determine the amount of copper remaining after sufficient time was allowed for loading.

Table C1: Batch Test Results Indicating Copper Levels (in ppm) Remaining in Solution

	PFC100 5g/L	PFC100 10g/L	PFC100 20g/L
pH 5.4	58.7	59.8	59.4
pH 6.2	59.1	59.0	59.1
No buffer	0.52	0.18	0.23
	PFC104 5g/L	PFC104 10g/L	PFC104 20g/L
pH 5.4	58.9	58.4	56.6
pH 6.2	58.5	57.9	55.7
No buffer	27.3	20.0	13.8
	S930 5g/L	S930 10g/L	S930 20g/L
pH 5.4	7.63	1.90	0.57
pH 6.2	6.11	0.99	0.26
No buffer	0.18	0.33	0.25
	S940 5g/L	S940 10g/L	S940 20g/L
pH 5.4	44.8	34.4	20.8
pH 6.2	35.5	20.0	6.3
No buffer	0.21	12.7	13.1
	MNP 5g/L	MNP 10g/L	MNP 20g/L
pH 5.4	57.9	57.2	56.7
pH 6.2	58.4	58.1	57.1
No buffer	<0.05	<0.05	<0.05

The S930 was the only resin that performed well in the citrate buffer solutions, but it was also observed that the same resin performed well in the unaltered 60 mg/L copper solution. To better endure the more acidic environment, additional process steps would be required to switch the resin from the as received Na⁺ form to the H⁺ form. PFC100 and MNP both performed significantly better when no citrate was present in solution. PFC100, S930, S940, and MNP were selected for column testing, based upon the results of the batch tests.

The equilibrium data was analyzed using the Langmuir adsorption model (see Appendix B, Equation 12). The ratio of copper in solution (C_e , mg Cu/L solution) to the amount of copper adsorbed per gram of resin (Q_e) was plotted versus the equilibrium copper concentration.

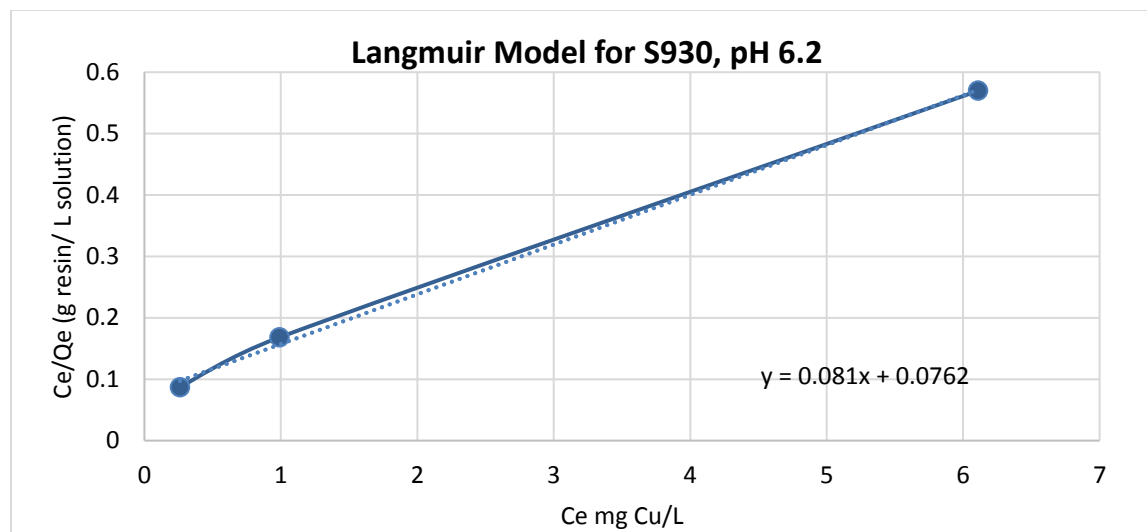


Figure C1: Langmuir adsorption model for the batch test results of S930, pH 6.2.

The parameters Q_m and K_{ads} were determined by fitting a trend line to the data points in Figure C1. Q_m was determined to be 12.35 mg Cu/g resin, and K_m was calculated to be 1.06 L/g. Table C2, compares the experimental results of C_e and Q_e with the results calculated from the model.

Table C2: Comparison of Experimental and Langmuir Model Equilibrium C_e and Q_e Values

		Model		Experimental	
Sample No.	Mass of Resin (g)	C_e (mg Cu/L)	Q_c (mg Cu/g resin)	C_e (mg Cu/L)	Q_c (mg Cu/g resin)
16	0.1005	6.170	10.712	6.11	10.724
17	0.2005	0.861	5.899	0.99	5.886
18	0.3998	0.300	2.986	0.26	2.988

Resins S930, S940, and PFC100 were evaluated to obtain kinetic data via column tests. The copper concentration for all three solutions was 1000 mg/L, and only the S930 column test was run with solution prepared from the 0.1 M citrate buffer. Atomic absorption (AA) spectroscopy was employed to analyze the aliquots collected from the experiments; the data for the three columns is presented in Figures C2-C4.

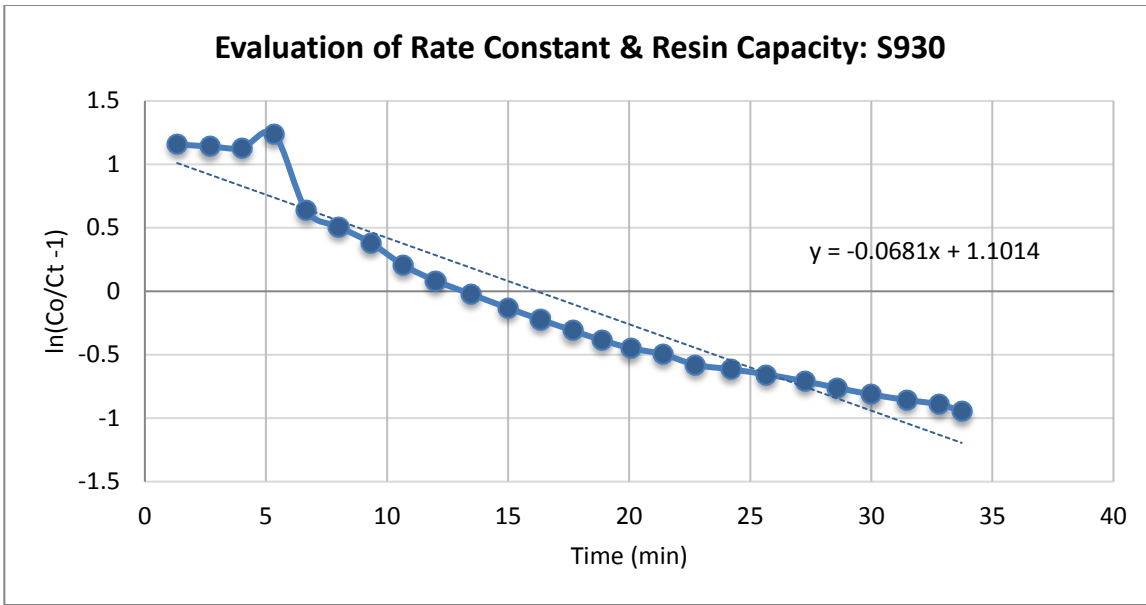


Figure C2: Linear trend of $\ln(C_o/C_t - 1)$ versus time for S930 column test.

The Thomas model (Appendix B, Equation 16) was employed to evaluate the kinetics of the column tests. From the linear trend line that was produced, the rate constant (k_1) was determined to be $6.93E-05 \text{ (mg/L)}^{-1} \text{ min}^{-1}$, and the resin capacity was determined to be 12.32 mg Cu/g resin.

The S930 loaded approximately 750 ppm of copper in the first 4.5 minutes of the column run time. As the solution continued to be pumped through the column, S930 adsorbed less copper; after 26 minutes, the resin only loaded 275 ppm of copper.

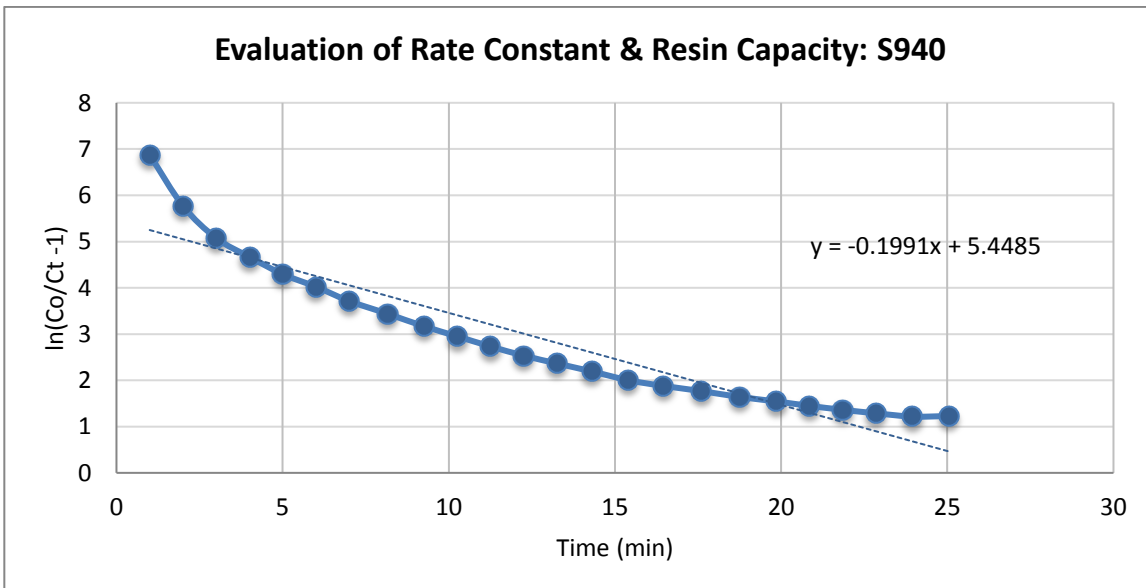


Figure C3: Linear trend of $\ln(C_o/C_t - 1)$ versus time for S940 column test.

From the equation generated in Figure C3, the rate constant for S940 was found to be $2.05\text{E-}04 \text{ (mg/L)}^{-1}\text{min}^{-1}$, and the resin capacity was determined to be $25.26 \text{ mg Cu/g resin}$. S940 loaded 966 ppm of copper within the first minute of the experiment. After six minutes only 17 ppm of copper was found to remain in the corresponding aliquot; even after 25 minutes had elapsed, S940 still adsorbed 748 ppm of copper onto the resin.

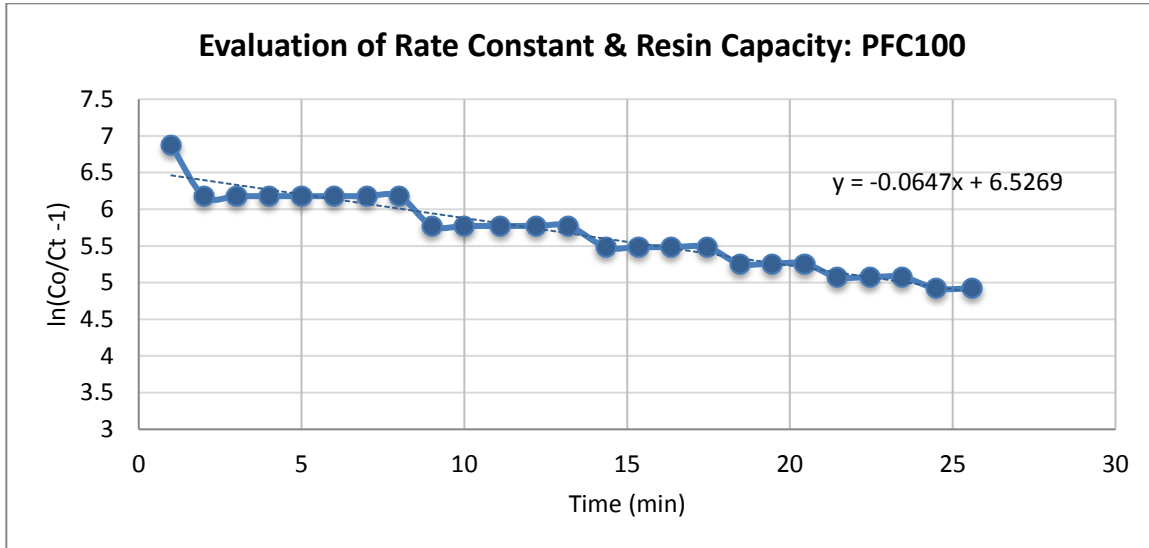


Figure C4: Linear trend of $\ln(C_0/C_t - 1)$ versus time for PFC100 column test.

The analysis of the PFC100 column data indicated that the rate constant was $6.69 \text{ (mg/L)}^{-1}\text{min}^{-1}$, and the resin capacity was $83.58 \text{ mg Cu/g resin}$. PFC100 adsorbed copper extremely well; unlike S930 and S940, the typical ‘S’ curve is not observed—additional time or a higher initial copper concentration would have allowed for this curve to develop. The resin consistently loads almost all of the copper from the solution passing through the column for the 25 minute duration.

Kinetic evaluation of the MNP was conducted via beaker tests, under the assumption that the adsorption of copper follows a pseudo-first order reaction mechanism.

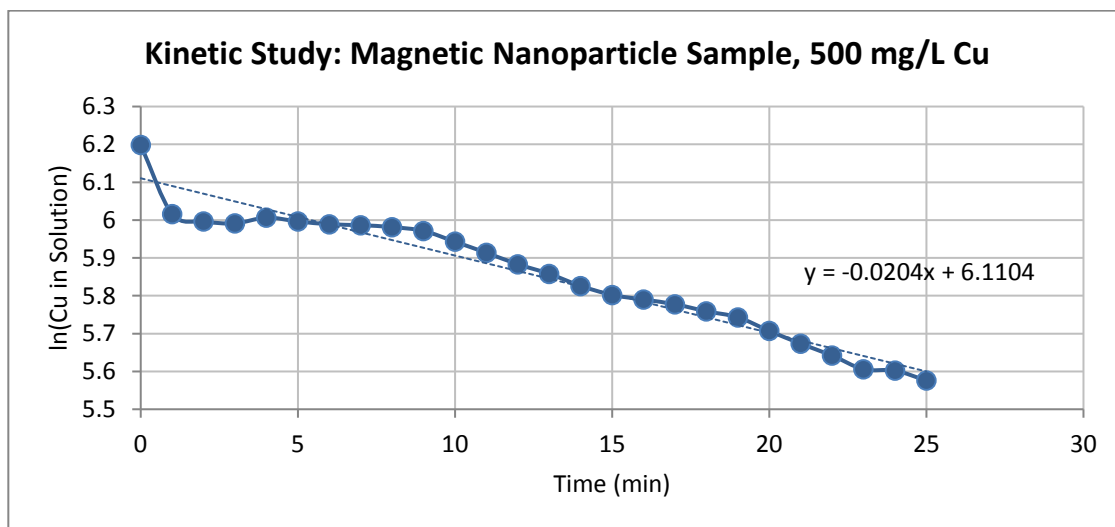


Figure C5: Copper remaining in solution as a function of time, MNP 500 mg/L beaker test.

The mechanism of the reaction is defined as:

$$\ln(C) = \ln(C_o) - k_1 t \quad (1)$$

The slope of the trend line provides the rate constant, and for the 500 mg/L beaker test the value of the rate constant was $2.04\text{E-}02 \text{ min}^{-1}$. In the first seven minutes of contact time, the UofM resin loaded only 94 ppm of copper. As the beaker test progressed, the resin continued to adsorb more copper from the solution, which was in contrast to the other three resins tested. At the end of 25 minutes, magnetic nanomaterial loaded 228 ppm of copper.

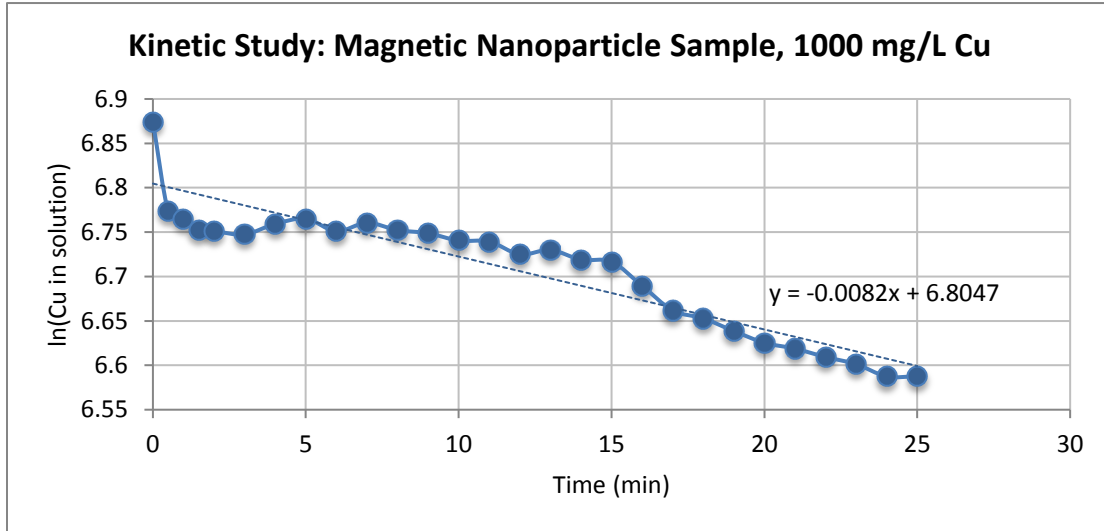


Figure C6: Copper remaining in solution as a function of time, MNP 1000 mg/L beaker test.

The rate constant for the 1000 mg/L beaker test was found to be $8.20\text{E-}03 \text{ min}^{-1}$. The UM particles loaded slightly over 100 ppm in the first seven minutes of the beaker test. Similar to the first beaker test, the UM particles continued to load as the experiment progressed. Once 25 minutes had elapsed, the resin adsorbed 241 ppm of copper.

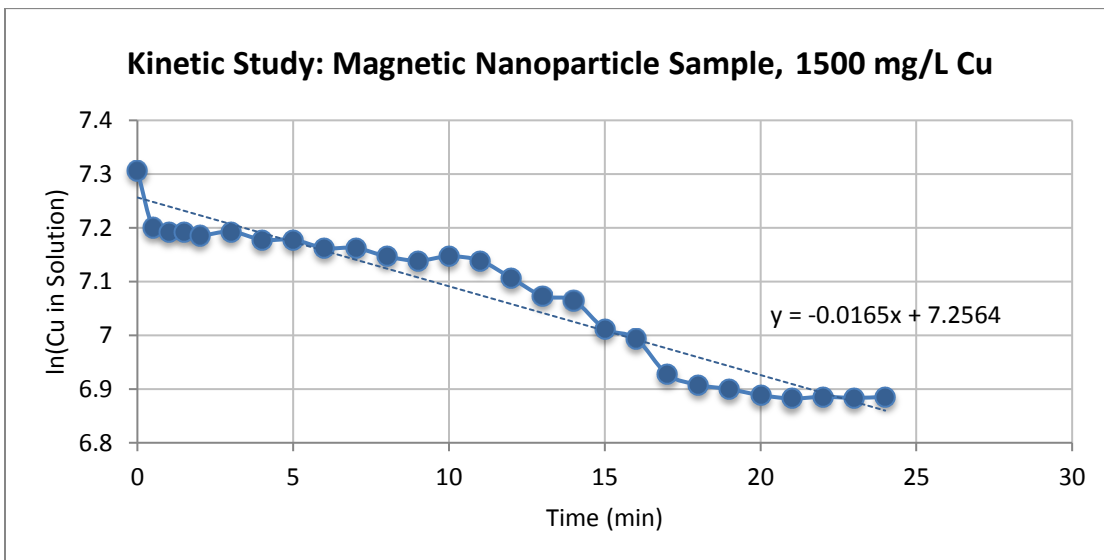


Figure C7: Copper remaining in solution as a function of time, MNP sample 1500 mg/L beaker test.

The final beaker test produced the data presented in Figure C7, and the rate constant of this test was determined to be $1.65\text{E-}02 \text{ min}^{-1}$. The MNP adsorbed 160 ppm of copper in the first three minutes of the beaker test utilizing the 1500 mg/L copper solution. The adsorption of copper onto the resin was very gradual until the 11 minute mark. The MNP particles loaded approximately 512 ppm of copper, over 25 minutes.

Conclusions

The results confirm the magnetic nanoparticles rapidly adsorb copper from solutions in the range of 100 ppm of copper within the first several minutes, which indicates that the resin is viable for wastewater sources with relatively low copper concentrations. Issues in handling the small particle size necessitated that kinetic studies be conducted via beaker tests rather than the traditional column method utilized for the commercial resins tested for comparison. On the other hand, PFC100 shows a great promise in terms of its loading capacity and its overall hardness as a strong acid resin. Each resin should be tested with actual mine wastewater samples to evaluate the effect of competing metal ions in solution. Additionally, column tests could also be performed to further investigate resin loading.

APPENDIX D

Dr. Katherine Zodrow

Assistant Professor, Montana Tech Department of Environmental Engineering

Ms. Christina Eggensperger

Graduate Research Assistant, Montana Tech Department of Environmental Engineering

Electrolyte Modeling

- OLI Stream Analyzer software was used to model the membrane distillation (MD) treatment processes of a copper sulfate solution to predict the likelihood of membrane scaling.
- Electrolyte analysis indicates that scale is likely to form at CuSO_4 concentrations > 0.4 M (64 g/L), much higher than the concentrations likely to be encountered in the MD system (Figure D1).

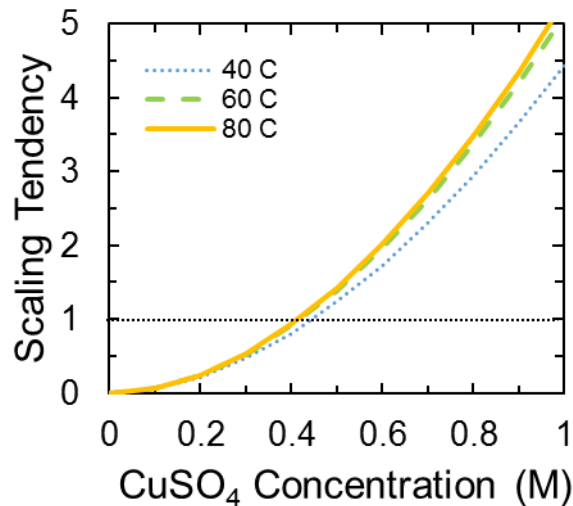


Figure D1. Copper sulfate solution concentration plotted against scaling tendencies. A scaling tendency ≥ 1 indicates that scale is likely to form at that concentration. Scaling tendency was calculated using OLI Stream Analyzer.

Membrane Distillation Performance

- Our direct contact membrane distillation operates with two closed loops separated by a hydrophobic, microporous membrane (Pall, 0.2 μm). Over time, the feed solution concentrates (becoming the “concentrate”) while distilled water passes to the distillate stream.
- MD was used to concentrate 5 L of 100mg/L copper sulfate solution 10x, reducing the total volume of copper sulfate solution to 0.5 L. Data collected includes temperatures of the inlets and outlets to the hot and cold sides of the MD module, time, and conductivity. Samples taken from the feed/concentrate and distillate reservoirs were acidified with 100 μL of HNO_3 for ICP-

OES analysis. Each experiment ran for at least 50 hours. After each experiment, the membrane was stored in a beaker of DI water for analysis.

- In MD, a decrease in flux through the membrane during the duration of the experiment is undesirable, as this would result in a decrease in performance. No significant decrease in flux was observed (Figure D2A).
- Analysis of the distilled water (ICP-OES) indicated an initial decrease in copper concentration and an increase in copper concentrations towards the end of the experiment (Figure D2B). The initial decrease is due to dilution of residual copper in the system at the beginning of the experiment. The increase in copper concentrations towards the end of the experiment is likely due to a small amount of membrane scaling and pore wetting. (The copper concentrations in the distillate are much lower than the EPA recommended water quality criteria for copper, 1.3 ppm.) No sulfate was detected in the distillate (detection limit: 0.07 ppm). Copper in the concentrate was observed to be ~70 ppm at the end of the experiment (Figure D2C).

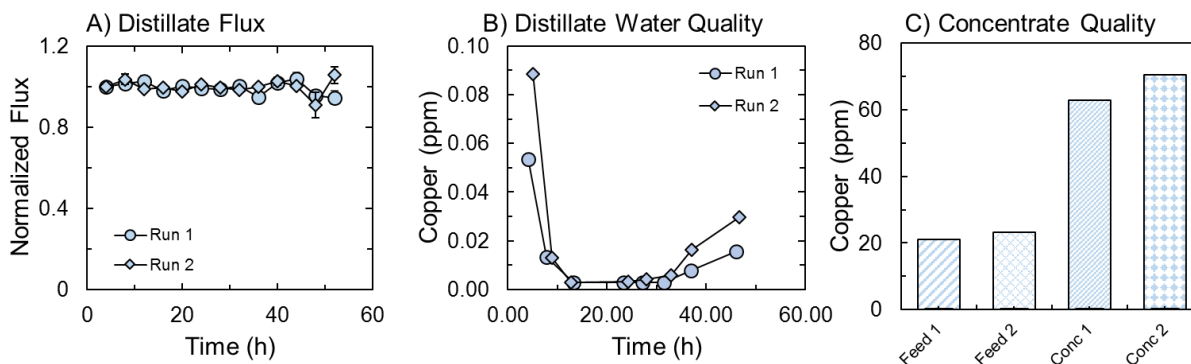


Figure D2. Performance of MD treating 100 mg/L copper sulfate: (A) normalized membrane flux over time. (B) copper concentrations in the distilled water reservoir; and (C) copper content in the feed and concentrate solutions. Membrane flux was normalized to the initial flux for Membrane 1 ($37.93 \pm 1.77 \text{ Lm}^{-2}\text{h}^{-1}$) and Membrane 2 ($44.9 \pm 1.28 \text{ Lm}^{-2}\text{h}^{-1}$). Temperatures at inlet and outlet of membrane module during experimentation were as follows: Membrane 1, Hot In: 52.8 ± 1.93 , Hot Out: 46.9 ± 1.40 , Cold In: 25.6 ± 1.98 , Cold Out: 23.0 ± 1.57 ; Membrane 2: Hot In: 53.7 ± 1.03 , Hot Out: 47.2 ± 0.76 , Cold In: 26.9 ± 1.21 , Cold Out: 24.0 ± 0.91 .

Measuring Membrane Pore-Wetting and/or Fouling

- In MD, the microporous hydrophobic membrane is filled with vapor. As water evaporates, non-volatile contaminants (e.g. copper sulfate) remain in the concentrate. As hydrophilic scale forms on the membrane, the membrane can wet, and water can enter the pores, allowing non-volatile contaminants to diffuse across the membrane. This will lead to a lower final concentration in the concentrate, and it may hinder downstream processes or environmental discharge of the distilled water.
- Used membranes were cut to fit inside an ultrafiltration cell (Amicon, EMD Millipore) to measure liquid entry pressure (LEP). LEP was also measured with a clean, unused membrane. LEP measures the amount of pressure required to force water into the pores of the membrane. As membranes wet, the LEP decreases. A significant decrease in LEP was observed on membranes treating copper sulfate, indicating that pore wetting had occurred (Figure D3A).

- Used membranes were cut into strips, and their water-in-air contact angle was measured using a ThetaLite contact angle goniometer. A smaller contact angle between a water droplet and a surface means that the surface is more hydrophilic rather than hydrophobic. Scaled MD membranes tend to have a somewhat lower contact angle (Figure D3B).

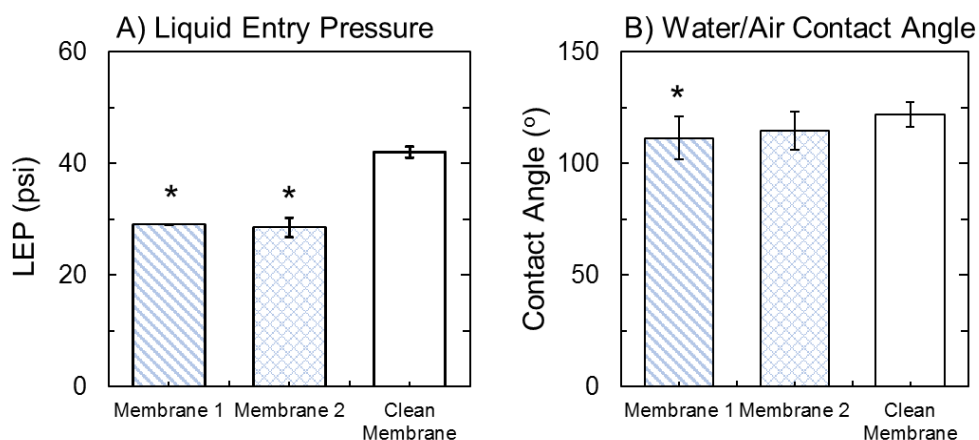


Figure D3. Membrane characterization: (A) LEP and (B) water-in-air contact angle of used membranes compared to a pristine control. An asterisk denotes a significant difference between the sample and the clean membrane.

Scale Characterization

- Dried membrane samples were used in x-ray diffraction (XRD) to determine the presence of crystalline structures that have scaled onto the membrane during experimentation (Figure D4A). The mineral observed resembled posnjakite, a copper sulfate derivative.
- Very little scale was observed on the membrane surface, as viewed using scanning electron microscopy (Figure D4B).

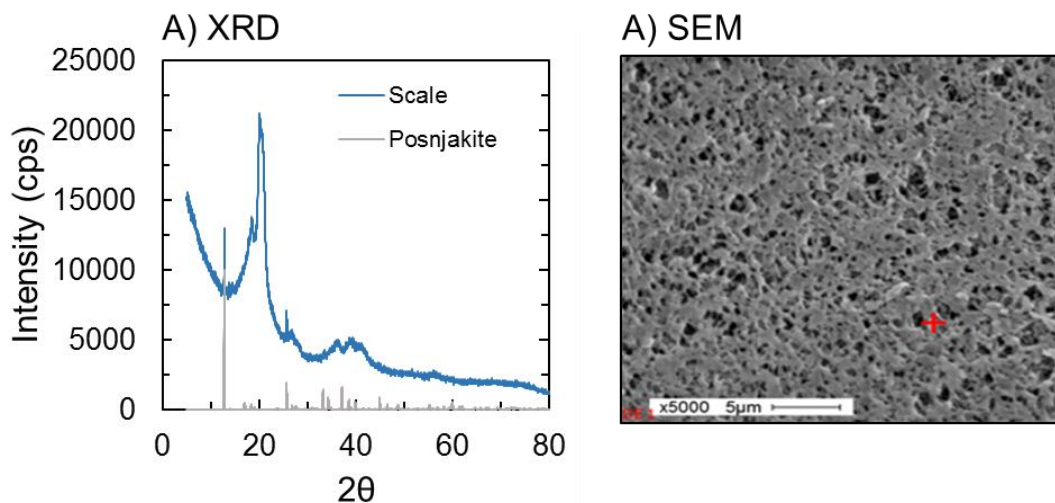


Figure D4. Membrane scale characterization: (A) XRD analysis of scale formed on membrane surface. The reference spectra shown for posnjakite was obtained from the RRUFF Project. (B) A scanning electron micrograph of a used membrane.